





Temperature and palaeolake evolution during a Middle Pleistocene interglacial–glacial transition at the Palaeolithic locality of Schöningen, Germany

KIM J. KRAHN , BRIGITTE URBAN, SYLVIA PINKERNEIL, DAVID J. HORNE, MARIO TUCCI, ANDREAS KOUTSODENDRIS  AND ANTJE SCHWALB

BOREAS



Krahn, K. J., Urban, B., Pinkerneil, S., Horne, D. J., Tucci, M., Koutsodendris, A. & Schwalb, A. 2024 (October): Temperature and palaeolake evolution during a Middle Pleistocene interglacial–glacial transition at the Palaeolithic locality of Schöningen, Germany. *Boreas*, Vol. 53, pp. 504–524. <https://doi.org/10.1111/bor.12670>. ISSN 0300-9483.

The Middle Pleistocene Reinsdorf sequence at the Lower Palaeolithic sites of Schöningen offers the opportunity to reconstruct a rarely well-preserved post-Holsteinian environmental transition from an interglacial into a glacial phase along with its highly dynamic interjacent climatic oscillations. Combining biological proxies, element composition and stable isotope ratios of two lakeshore sequences at excavation site 13 II, we demonstrate repeated variations in climate, hydrology and catchment vegetation cover. New ostracod-based quantitative mean summer and winter air temperature reconstructions with the Mutual Ostracod Temperature Range (MOTR) method provide the first detailed information about the temperature evolution. The interglacial temperature maximum, probably corresponding to Marine Isotope Stage 9e, is followed by a first dry phase and, during the younger part of the Reinsdorf sequence, by a second dry period. Both were marked by lower precipitation/evaporation ratios, reduced vegetation cover in the catchment and increased surface inflows from springs. Temperature reconstructions of these two steppe (open woodland) phases yield very narrow ranges for mean January (−4–0 °C) and July (+17–19 or +17–21 °C) air temperatures, demonstrating that, while summers were similar to those of today, winters were at least 1 °C colder, hinting at a more pronounced continental climate. Precise temperature estimates for the interjacent woodland and steppe (woodland) phase are hindered by generally wider ranges produced by the MOTR method (January mean −4–3 °C, July mean +15–21 °C). The development of a more extensive vegetation cover, reducing surface runoff and erosion in favour of increased river and groundwater discharge, as indicated by a shift in microfossil and stable isotope records, suggests generally more humid climates with higher precipitation/evaporation ratios as well as reduced seasonal temperature variations.

Kim J. Krahn (k.krahn@tu-braunschweig.de) and Antje Schwalb, Technische Universität Braunschweig, Institute of Geosystems and Bioindication, Langer Kamp 19c, 38106 Braunschweig, Germany; Brigitte Urban and Mario Tucci, Leuphana University Lüneburg, Institute of Ecology, Landscape Change, Universitätsallee 1, 21335 Lüneburg, Germany; Sylvia Pinkerneil, GFZ German Research Centre for Geosciences, Climate Dynamics and Landscape Evolution Section, Telegrafenberg, 14473 Potsdam, Germany; David J. Horne, Queen Mary University of London, School of Geography, Mile End Road, London E1 4NS, UK and Earth Sciences Department, The Natural History Museum, Cromwell Road, London SW7 5BD, UK; Andreas Koutsodendris, Institute of Earth Sciences, Heidelberg University, Im Neuenheimer Feld 234, 69120 Heidelberg, Germany; received 29th December 2023, accepted 13th June 2024.

In light of current climate change, Middle Pleistocene interglacials have attracted increasing interest because they provide information about past climate dynamics (Tzedakis *et al.* 2009). These periods can be regarded as natural climate variability analogues to the current interglacial, the Holocene, giving insights into present-day, anthropogenically driven climate warming, and can be used for developing more reliable climate scenarios (Berger & Loutre 2003; Thompson 2004; Schulz & Paul 2015; Yin & Berger 2015). In particular, Marine Isotope Stage (MIS) 11 has become the centre of attention because of its similarities to the Holocene in terms of low-amplitude insolation variations (Loutre & Berger 2003; Candy *et al.* 2014; Past Interglacials Working Group of PAGES 2016; Tzedakis *et al.* 2022). The investigation of other stages such as MIS 9, however, offers the opportunity to evaluate the evolution of interglacial periods influenced by different boundary conditions and the variable response of the climatic system. More importantly, MIS 9 is considered one of the

best analogues of the Holocene because: (i) its caloric summer half-year insolation is the closest to that of the Late Holocene throughout the last ~450 000 years (Ruddiman 2007); and (ii) it is marked by the highest pre-industrial atmospheric carbon dioxide concentrations of the past 800 000 years, as documented by the Antarctic ice core record (Lüthi *et al.* 2008).

Although several continental records are available for MIS 9 from Europe, for example, speleothem records (Berstad *et al.* 2002; Drysdale *et al.* 2004; Regattieri *et al.* 2018; Błaszczyk & Hercman 2022) and sediment records (Reille *et al.* 2000; Lacey *et al.* 2016; Koutsodendris *et al.* 2023), only a few offer quantitative temperature reconstructions (e.g. Bridgland *et al.* 2013). On this basis, MIS 9 is the least investigated of all late Middle Pleistocene interglacials, so insights into the response of ecosystems to the special climate characteristics of MIS 9 (e.g. high obliquity, high CO₂ concentration; Yin & Berger 2015) are limited and further data therefore much needed. What is known, however, is that the MIS 9

interglacial–glacial transition has been punctuated by several suborbital cold events in the North Atlantic Ocean and its borderlands (Martrat *et al.* 2005, 2007; Roucoux *et al.* 2006; Desprat *et al.* 2009). These episodes were proposed to be related to changes in the deep-water circulation and partly to iceberg discharges (Desprat *et al.* 2009). Changes in the North Atlantic drift have substantially affected central Europe's climate during the late Eemian (Sirocko *et al.* 2005), and it stands to reason that the MIS 9 North Atlantic cooling episodes might have left an imprint as well.

In central Europe, near- and long-distance correlation of interglacial records, post-dating the Elsterian and pre-dating the Saalian Drenthe stadial, with other terrestrial records and the marine oxygen isotope record is still under debate (Lauer & Weiss 2018). Few terrestrial, stratigraphically well referable deposits are preserved at, for example, Munster-Brelloh (Müller 1974), Dethlingen (Koutsodendris *et al.* 2010), Leck (Stephan *et al.* 2011) and Ummendorf (Strahl 2019; Wansa *et al.* 2019). The number of non-Holsteinian sequences (from Schöningen: Urban *et al.* 1991; Urban 1995, 2007; from Pit Nachtigall: Kleinmann *et al.* 2011; Waas *et al.* 2011) is still low (Nitychoruk *et al.* 2006) and their chronostratigraphical position under discussion, which emphasizes the need for well-preserved, dated sequences enabling both a better correlation of central European sites and reinforcement of the chronostratigraphical positions.

Covering several interglacial–glacial cycles, the open-cast lignite mine of Schöningen, Germany is of great interest for Middle Pleistocene stratigraphy as it represents a comprehensive climatic archive excellently suited for multidisciplinary research (Thieme 2007; Urban *et al.* 2011; Conard *et al.* 2015; Serangeli *et al.* 2018). Abundant archaeological finds at the Lower Palaeolithic sites, for example the worldwide oldest wooden hunting spears (Thieme 2007), additionally enable direct correlation of environmental change and human habitats. The spears were deposited in a post-Elsterian interglacial–glacial sequence, which, based on palynological data, shows differences from Holsteinian deposits found in Schöningen and other sequences of the Holsteinian Interglacial; therefore, the initially only exposed interglacial section of the Reinsdorf sequence was named the Reinsdorf Interglacial (Urban 1995). Some authors, however, have considered the Reinsdorf Interglacial as a regional variety of the Holsteinian *sensu stricto* (Litt *et al.* 2007; Bittmann 2012). Moreover, the general correlation of the Holsteinian Interglacial with MIS 11 (e.g. Nitychoruk *et al.* 2005; Candy *et al.* 2014; Cohen & Gibbard 2016) or, alternatively, with MIS 9 (Geyh & Müller 2005; Geyh & Krbetschek 2012) remains controversial, although detailed investigation of a pollen record from Dethlingen suggests an allocation of the Holsteinian to MIS 11c (Koutsodendris *et al.* 2010). The correlation of biostratigraphically clearly assigned Holsteinian deposits to MIS 11 was

recently confirmed by tephrochronological data from the Eifel region (Fernández Arias *et al.* 2023). Based on thermoluminescence dating of heated flints from deposits of the archaeological site Schöningen 13 I, which lies stratigraphically below the Reinsdorf deposits, a correlation with MIS 9 was proposed for the Reinsdorf sequence (Richter & Krbetschek 2015). Recently obtained ages of about 300 ka for sediments from a new find horizon within the sequence, based on luminescence dating, further support this correlation (Tucci *et al.* 2021). Therefore, results strengthen a separation into two different interglacial periods, supporting a correlation of the Holsteinian with MIS 11, and of the Reinsdorf with MIS 9. Because of the characteristic climatic dynamics and short-term oscillations of the individual marine isotope stages and corresponding interglacial stages in Europe (Martrat *et al.* 2005; Desprat *et al.* 2009; Koutsodendris *et al.* 2011, 2013), additional information about the climatic evolution of the Reinsdorf sequence is important to further confirm its stratigraphical position as well as the chronological position of its oscillations.

Although multi-proxy data about the environmental developments during the Reinsdorf sequence are already available (e.g. van Kolfshoten 2014; Böhme 2015; Urban & Bigga 2015; Krahn *et al.* 2021; Urban *et al.* 2023a), detailed temperature reconstructions are still missing, and continuous interpretations are hindered by changing preservation of aquatic fossil remains and depositional gaps or poorly developed levels of previously investigated sequences, as well as lower sampling resolution. For this study, we analysed ostracods and diatoms that have been widely used to reconstruct past temperatures (Horne *et al.* 2012), water depths (Wrożyna *et al.* 2009) and salinities (Gasse *et al.* 1987; Kashima 2003), among others. They are often well and abundantly preserved in lake sediments and show great sensitivity to environmental variations. Biological proxies, together with geochemical proxies, preserved in lacustrine sequences can yield high-resolution large-scale to site-specific palaeo-environmental information (Last & Smol 2001; Smol *et al.* 2001a, b). Here, elemental composition (total organic carbon (TOC), CaCO₃ and C/N ratios) and stable isotopes of bulk carbonates ($\delta^{13}\text{C}_{\text{carb}}$, $\delta^{18}\text{O}_{\text{carb}}$) and ostracod valves ($\delta^{13}\text{C}_{\text{ostracod}}$, $\delta^{18}\text{O}_{\text{ostracod}}$), combined with microfossil analyses, were performed to trace variations in temperature, hydrology and catchment development more precisely. Two lakeshore sequences from archaeological site Schöningen 13 II were selected to distinguish between sequence-specific signals and to overcome the aforementioned limitations.

This study integrates qualitative as well as quantitative biological and geochemical data. Our aim is (i) to develop a detailed quantitative temperature reconstruction and (ii) to contribute to a better understanding of the Reinsdorf post-interglacial climate oscillations and thereby aquatic ecosystem responses during MIS 9 in central Europe. Mutual Ostracod Temperature Range (MOTR) method results and the inferred climatic

oscillations are compared with published data from European Middle Pleistocene MIS 9 records in order to (iii) test the proposed chronological position of the Reinsdorf sequence.

Site description

The excavation sites of Schöningen (latitude 52°8' N, longitude 11°0' E; 90–130 m a.s.l.) are located in a former open-cast lignite mine about 100 km east of Hanover in northern Germany (Fig. 1A). Today, the 20-year average mean air temperature of the coldest month (January) in the Schöningen area is 1.0 °C, and that of the warmest month (July) is 18.8 °C (DWD 2003–2022; station: Ummendorf Helmstedt). Annual precipitation amounts to 531 mm per year (DWD 1988–2022; station: Ummendorf Helmstedt). Precipitation is highest during the summer months (June, July, August), and $\delta^{18}\text{O}$ values of January precipitation are about 3‰ more negative compared with those of July precipitation (IAEA/WMO 2022).

The lignite seams and overlying deposits were deposited within a rim syncline, developed along the edge of the Helmstedt–Staßfurt salt wall, a 70-km-long narrow salt structure, which runs along the north-eastern area of the mine in a NW–SE direction (Brandes et al. 2012). The Elm, a small mountain ridge composed of Muschelkalk limestone, is situated NW close to the study site (Fig. 1B), and waters from its springs reach the decommissioned lignite mine from the

west and through the stream Missaue from the north (Evers 2017). Several archaeological sites were identified in Schöningen, of which especially site 13 II yielded many important Palaeolithic finds (Thieme & Mania 1993; Thieme 1997; Serangeli et al. 2012).

Overlying Elsterian till, a sequence of six superimposed interglacial–glacial cycles was identified and interpreted as infillings of NW- to SE-trending large-scale fluvial channels (Mania 1995, 2007). This model, although challenged by other authors (Lang et al. 2015), provides the nomenclature of the individual sites (channels I–VI). Each cycle starts with late glacial sediments, which are discordantly overlain by silty, organic-rich limnic–telmatic sediments, and encompass an interglacial phase and its transition into a succeeding glacial period. More recently, deposition of the sequences within an elongated lake basin, formed in the depression of an Elsterian tunnel valley, was inferred based on data from outcrop sections, borehole logs and shear wave seismics (Lang et al. 2012, 2015). The channels were interpreted as major unconformities within a palaeodelta caused by climate-driven lake level variations. Site 13 II was proposed to be located on a delta plain along the southwestern shore of a long-lived palaeolake fed by small streams from the Elm.

Based on palynological evidence, Urban et al. (1988, 1991), Urban and Thieme (1991) and Urban (1995) defined three succeeding interglacial–glacial cycles sandwiched between the Elsterian and Saalian glacial deposits. The oldest deposits (channel I) were assigned to the Holsteinian Interglacial, whereas the deposits of

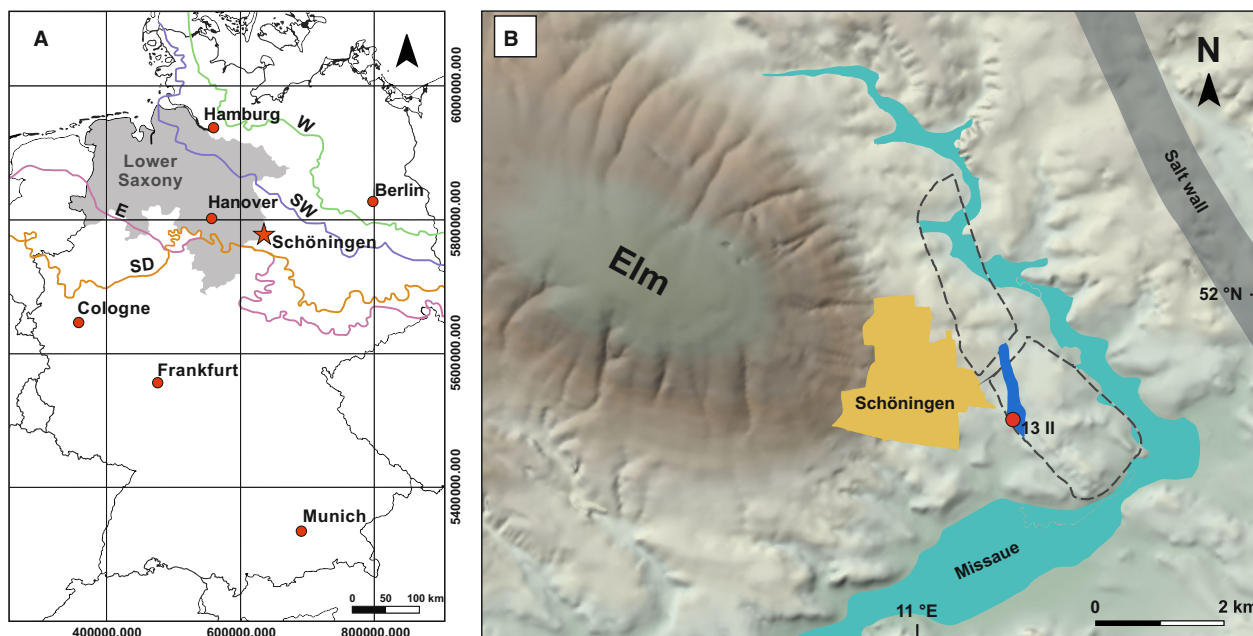


Fig. 1. A. Location of Schöningen (star) in Germany. Coloured lines indicate the maximum extent of Pleistocene ice sheets (E = Elsterian; SW = Saalian Warthe ice advance; SD = Saalian Drenthe ice advance; W = Weichselian) (modified from Tucci et al. 2021). B. Digital elevation model showing the Elm and direct surroundings, city of Schöningen, salt wall, position of the open-cast mine (dashed lines) with archaeological site 13 II (red dot), the modern Missaue flood plain and spatial distribution of the Reinsdorf deposits (blue area) (modified from Serangeli et al. 2018; original map by U. Böhner, NLD, Hanover; DEM by D. Fabian).

channel II were locally defined as the Reinsdorf Interglacial (Urban *et al.* 2011; Sierralta *et al.* 2012; Urban & Bigga 2015). Deposits from the northern mining area representing the pollen succession of channel III were named the Schöningen Interglacial and correlated with MIS 7, based on palynological data (Urban *et al.* 1991; Urban 1995, 2007).

Material and methods

Sampling of the two Reinsdorf sequences

Two sequences were sampled at archaeological site 13 II (Fig. 1B). Sequence one, consisting of two profiles, Para-Reference Profile (PRP) 13 II (2014) (13 II-2c5-II-4e1) and Zeugenblock (ZB) 13 II (2018) (13 II-4c-II-5c3), was sampled in 2014 and 2018, respectively. Both profiles were combined in order to cover the whole Reinsdorf sequence, and had a total thickness of about 6.3 m. A detailed lithological description of this sequence is given in Urban *et al.* (2023a). Sequence two, Reference Profile (RP) 13 II (2003) (13 II-1c4-II-5c2), had already been sampled in 2003. From five staggered profiles, samples were taken using 25 × 7 × 5-cm-sized steel boxes for palynological and geochemical analyses (Urban & Bigga 2015). Previously recovered ostracod valves from subsamples thereof (Krahn *et al.* 2021) were analysed for MOTR and stable isotopes in this study. Samples of the combined sequence PRP 13 II (2014)/ZB 13 II (2018) had a resolution of 1 cm, while samples from sequence RP 13 II (2003) were generally integrated 1–2 cm. The designation (13 = archaeological site; II = channel/climatic cycle) and subdivision (level, II-1 to -5; sublevel, II-1a; sub-sublevel, II-1a1) used in this study follow Mania (1998), Böhner *et al.* (2005) and Urban and Bigga (2015).

Ostracod analyses

Ninety-one samples from sequence PRP 13 II (2014)/ZB 13 II (2018) were analysed for ostracods (resolution on average 7 cm). For each sample, between ~2 and 8 g of sediment was processed. Samples were immersed overnight in ~4% H₂O₂ to remove organic matter and subsequently washed through stacked mesh sieves (250, 125 and 63 μm) to separate the sample in different size fractions. If possible, up to ~300 valves were picked from the 250-μm fraction using fine brushes. Specimens were identified under a Leica M80 stereoscopic microscope. In the two smaller fractions, valves were counted to assess the ostracod concentration. Taxonomic identification of ostracods is based on standard identification keys (Meisch 2000; Fuhrmann 2012).

Diatom analyses

A total of 36 samples (resolution on average 18 cm) from sequence PRP 13 II (2014)/ZB 13 II (2018) were prepared

for diatom analysis after Kalbe and Werner (1974) with minor modifications. Naphrax[®] was used as the mountant to prepare permanent slides and diatom valve counting was performed using a Leica DM 5000 B LM, equipped with a ProgRes[®] CT5 camera with differential interference contrast under oil immersion at ×1000 magnification. The diatom concentration was determined by adding known quantities of polystyrene microspheres to the processed sample (Battarbee & Kneen 1982). If possible, 400 valves per sample were identified using standard literature (Krammer & Lange-Bertalot 1986, 1988, 1991a, b; Lange-Bertalot *et al.* 2017) along with relevant taxonomic publications. In samples with low diatom concentration, diatoms were analysed until 1000 microspheres had been counted. In samples lacking diatoms or with very low diatom concentration, analyses were stopped when 500 microspheres and not more than 10 diatom valves had been counted.

Elemental and stable isotope analyses of bulk sediments and ostracod valves

In total, 89 samples of sequences PRP 13 II (2014)/ZB 13 II (2018) were analysed (resolution on average 7 cm). Total carbon (TC), total nitrogen (TN) and TOC were determined on ground bulk samples using an elemental analyser (FlashEA 1112), connected with a ConFloIV interface on a DELTA V Advantage IRMS (isotope ratio mass spectrometer, ThermoFischer Scientific) at the GFZ German Research Centre for Geosciences in Potsdam, Germany. For TC and TN on average 2 and 40 mg, respectively, sample material was loaded into tin capsules and burned in the elemental analyser. The calibration for TC and TN was performed using urea and acetanilide, respectively. The calibration was checked with a soil reference sample (Boden3, HEKATECH). Replicate determinations show a standard deviation better than 0.2% for TC and TN.

The TOC contents were determined on *in-situ* decalcified samples. About 3 mg of sample material were weighted into Ag capsules, drizzled first with 3% and second with 20% HCl, heated for 3 h at 75 °C, and finally wrapped into the Ag capsules and measured, as described above. The calibration was performed using urea and checked with a soil reference sample (Boden3, HEKATECH). The reproducibility for replicate analyses is 0.2%. The CaCO₃ content was calculated using the equation (TC – TOC) × 8.33. To calculate C/N ratios, TOC values were divided by TN values.

Bulk carbonate samples [PRP 13 II (2014)/ZB 13 II (2018) + 51 samples of RP 13 II (2003)] and cleaned ostracod valves [only RP 13 II (2003)] were analysed for δ¹³C and δ¹⁸O using a Finnigan MAT253 mass spectrometer connected to an automated carbonate-reaction device (KIEL IV). Samples of around 80 μg for ostracod valves and around 0.2 mg for bulk analyses were automatically dissolved with 103% H₃PO₄ at 72 °C, and the isotopic

compositions were measured on the released and cryogenically purified CO₂. The isotope composition is given in the delta notation relative to VPDB (Vienna Peedee Belemnite). Replicate analysis of reference material (NBS19, internal C1) yielded standard errors of <0.07‰ for both δ¹³C and δ¹⁸O. Because not sufficient adult valves of one single ostracod species in sequence RP 13 II (2003) were available throughout the entire sequence, stable oxygen and carbon isotopes of ostracod valves were measured on juvenile *Candona* spp., which provided enough material for the analyses. Up to 15 valves were selected per sample, depending on their size and combined weight. As preparation for stable isotope measurements, valves were carefully cleaned under a binocular microscope using a fine brush, distilled water, ethanol and a 2% H₂O₂ solution. The δ¹⁸O values of juvenile *Candona* spp. valves were later corrected for the vital offset using the coefficient +2.2‰ VPDB (von Grafenstein et al. 1992, 1999).

Temperature reconstruction, data handling and visualization

Past mean January and July air temperature ranges were reconstructed by applying the MOTR method (Horne 2007; Horne et al. 2012; D.J. Horne unpublished data, Table S1) to both Reinsdorf sequences. Reconstructed ranges were compared with modern January and July temperatures for the locality, obtained from local weather stations (January +1 °C, July +18.8 °C) as well as with the WorldClim temperature data which are interpolated from climate data for the 50-year period 1950–2000 (January 0 °C, July +18 °C) and were used for the MOTR calibrations. The three-point moving average method was applied to the MOTR results to smooth short-term fluctuations and emphasize long-term trends (see Marchegiano et al. 2020). Samples that contained fewer than 10 identified ostracod valves (nine samples) and fewer than 25 identified diatom valves (four samples) were excluded from abundance analyses. Stratigraphical diagrams were created with C2 version 1.7.7 (Juggins 2007). Biplots, correlation analyses and three-point moving-averages were prepared using the program PAST version 3.25 (Hammer et al. 2001).

Results

Changes in the aquatic microfossil and geochemistry record of sequence PRP 13 II (2014)/ZB 13 II (2018)

Ostracod (0–787 valves g⁻¹ dry weight (DW)) and diatom (0–59 × 10⁶ valves g⁻¹ DW) concentration and preservation vary considerably throughout the sequence. In total, 45 ostracod and 17 diatom samples were void of microfossil remains. The ostracod assemblage is dominated by juvenile Candonidae (19.0–82.9%) and *Cyclopypris* taxa (0.5–57.1%), while *Ilyocypris bradyi* (2.0–36.7%), *Pseudocandona compressa* (0.3–16.8%), *Limnocythere inopinata* (0.4–

19.6%) and *Prionocypris zenkeri* (2.9–48.1%) are commonly present. In the diatom assemblage, small tycho-planktonic fragilarioid species (e.g. *Pseudostaurosira brevistriata*, *Pseudostaurosira elliptica*, *Punctastriata lancettula*, *Staurosira venter* and *Nanofrustulum sopotensis*) are dominant (10.3–81.2%). The diatom species *Navicula oblonga*, *Cymbopyleura inaequalis* and *Halamphora veneta* as well as the genera *Navicula*, *Epithemia* and *Cocconeis* are frequently found in the benthic community (17.9–70.6%) (Figs 2, S1).

The CaCO₃ content varies between 0 and 67% (mean 18%) and demonstrates a close relation to the ostracod concentration (Fig. 2). The TOC ranges between 1.3% (13 II-2c3) and 38.5% (13 II-2ab) and has a mean value of 8.7%. The C/N ratios exhibit the highest values in 13 II-2bc–II-3b1 (>20), while the lowest value (11) is found at the very top of the sequence (mean 16). δ¹³C_{carb} varies between -7.6 and -2.6‰ (mean -4.5‰), and δ¹⁸O_{carb} exhibits values between -9.8 and -7.3‰ (mean -8.1‰). Both parameters show the lowest values in layer 13 II-3b and the highest values in 13 II-4c.

Based on distinctive changes in the aquatic microfossil record (composition and frequency of occurrences), complemented by the palynology-based biostratigraphical record of Schöningen 13 II (Urban et al. 2023a), seven development zones (Z-I–VII) and an additional six subzones in zone IV (Z-IVa–IVf) were identified (Fig. 2, Table 1).

Zone I (13 II-2c5–II-2c4/5) did not yield any aquatic microfossil remains or carbonate. The TOC (7.1–11.4%) shows a decreasing trend. Zone II covers sub-sublevel 13 II-2c4. Ostracods, mainly juvenile Candonidae and *I. bradyi*, appear for the first time. The geochemical record does not display major variations. Zone III extends from sub-sublevel 13 II-2c3 to II-2c1. Ostracods are frequent in low concentrations (up to 100 valves g⁻¹ DW). *Cyclopypris* spp. (0–31.4%), *I. bradyi* (0–35.7%) and *P. zenkeri* (0–20%) increase in abundance. The TOC contents are low, CaCO₃ values are on average 13% and C/N ratios range between 13 and 18. The δ¹³C_{carb} (-5.4 to -4.5‰) and δ¹⁸O_{carb} (-7.9 to -7.4‰) exhibit only small variations.

Zone IV covers sublevels 13 II-2bc–II-4e1 and is divided into six subzones (Z-IVa–f) mainly based on diatom and ostracod developments. Although varying, the C/N ratios are higher and display a general decline (13–23) throughout Z-IV. Zone IVa (13 II-2bc) is again void of aquatic microfossils. The highest TOC contents of the whole sequence (38.5%), along with increasing C/N ratios (17–23), are recorded. In Z-IVb (13 II-3bc–II-3b2); ostracods are present in low concentrations (up to 62 valves g⁻¹ DW). Mostly valves of juvenile Candonidae were identified. The TOC decreases to an average of 16.9%. In Z-IVc (13 II-3b1 to lower part II-3b/3a) diatoms appear for the first time in low numbers and ostracods are absent. Benthic taxa dominate (up to 70.6%), although small tycho-planktonic fragilarioid diatom species are commonly (on average 22.4%)

Fig. 2. Synthesis diagram of the merged sequence Para-Reference Profile 13 II (2014)/Zeugenblock 13 II (2018) showing numbers of identified ostracod valves, ostracod concentrations, percentages of the most important ostracod taxa, diatom numbers and concentrations, abundances of small fragilarioid (yellow) and benthic (green) diatom taxa, along with results of geochemical analyses of sediments for TOC, CaCO₃, C/N, $\delta^{13}\text{C}_{\text{carb}}$ and $\delta^{18}\text{O}_{\text{carb}}$, and the identified development zones (Z). Grey lines in pollen ratio and geochemical data columns show mean values. Background colouring corresponds to reconstructed vegetation changes (orange, early- and late-temperate interglacial, thermophile, deciduous-dominated forests; light/dark green, post-temperate interglacial (boreal) forests and post-interglacial woodland and steppe (woodland); blue, post-interglacial steppe (open woodland); biostratigraphic subdivision, pollen data, palynological interpretation, and lacustrine sediment type from Urban *et al.* 2023a, see Table 1). The star indicates the level corresponding to the position of the archaeological 'spear horizon' of site 13 II. For this graphic representation, the pollen ratio from the sum of all woody plants and shrubs in relation to the Poaceae was used. This form of representation shows clearly that these are drought-loving grasses and not moisture-loving grasses (such as reeds, etc.), as they are dominant in the phases with low water levels as well as with other biological indicators of drought and, as reconstructed in Urban *et al.* (2023a, b), characterize the herbaceous grass-rich steppes and forest steppes.

observed as well. Ostracods are again present starting in Z-IVd (upper part 13 II-3b/3a to the beginning of II-4e3), and concentrations increase and reach a maximum of 579 valves g⁻¹ DW, while diatoms occur in concentrations up to 58.6×10^6 valves g⁻¹ DW. Correspondingly, CaCO₃ contents are high (up to 64%). The ostracod *P. compressa* occurs more frequently (up to 16.7%), while *P. zenkeri*, previously common in Z-III, is absent. The $\delta^{13}\text{C}_{\text{carb}}$ and $\delta^{18}\text{O}_{\text{carb}}$ drop in the beginning (minimum of -7.6 and -9.8‰ , respectively) and increase to values of -3.9‰

($\delta^{13}\text{C}_{\text{carb}}$) and -8‰ ($\delta^{18}\text{O}_{\text{carb}}$) in sublevel 13 II-4 g. The following Z-IVe (upper section of 13 II-4e3 to lower section of II-4e1) is distinguished by the new absence of microfossil remains. The TOC (on average 3.7%) and CaCO₃ (on average 2%) values are relatively stable and remain low. No diatoms are found in the uppermost samples of sub-sublevel 13 II-4e3 (Z-IVf) whereas ostracods increase in abundance (14–130 valves g⁻¹ DW). The highest recorded absolute abundances of *P. zenkeri* are found within Z-IVf (48.1%).

Table 1. Layers, development zones, biostratigraphic subdivision, and vegetational phases (Urban *et al.* 2023a) of the Para-Reference Profile (PRP) 13 II (2014) and Zeugenblock (ZB) 13 II (2018) of the Reinsdorf sequence. Two alternative stratigraphical positions (scenarios 1 and 2) with a tentative correlation of the Reinsdorf climatic oscillations with the Marine Isotope Stratigraphy (MIS) (Lisiecki & Raymo 2005), the north-western Iberia forest reduction events (NWI-fr) (Desprat *et al.* 2009) and the Iberian Margin Stadials (IMS) (Martrat *et al.* 2007) are presented.

Layer of PRP 13 II (2014)/ZB 13 II (2018)	Zone	Biostratigraphic subdivision of the Reinsdorf sequence (Urban <i>et al.</i> 2023a)	Vegetational phases of the Reinsdorf sequence (Urban <i>et al.</i> 2023a)	Scenario 1: tentative correlation with MIS, IMS and NWI	Scenario 2: tentative correlation with MIS, IMS and NWI
II-5c3	Z-VII	Reinsdorf E	Post-interglacial – early steppe-tundra phase	8c	9c
II-5d2	Z-VI	Reinsdorf D	Second post-interglacial woodland phase	9a	9d
II-4a/b	Z-V	Reinsdorf C	Second post interglacial – steppe (open woodland) phase	9b	3IMS-14 3NWI-fr3
II-4c	Z-IVf	Reinsdorf B3	Late First post-interglacial – woodland and steppe (woodland) phase	9c	9d
Uppermost part of II-4e1	Z-IVe				
Lower part of II-4e1					
Upper part of II-4e3	Z-IVd	Reinsdorf B2	Middle	3IMS-12 3NWI-fr6	
Lowermost part of II-4e3					
II-4ef					
II-4f					
II-4 g					
II-4 h1					
II-4 h2					
II-4i					
II-3ab	Z-IVc	Reinsdorf B1	Early	9c	
II-3b1	Z-IVb				
II-3b2					
II-3b3					
II-3bc					
II-2bc	Z-IVa				
II-2c1	Z-III	Reinsdorf A	First post-interglacial steppe (open woodland) phase	9d	3IMS-15 3NWI-fr2
II-2c2					
II-2c3					
II-2c4	Z-II	Reinsdorf Interglacial	Post-temperate interglacial zone (forest phase)	9e	9d
II-2c4/5	Z-I		Late-temperate interglacial zone (forest phase)		9e
II-2c5					

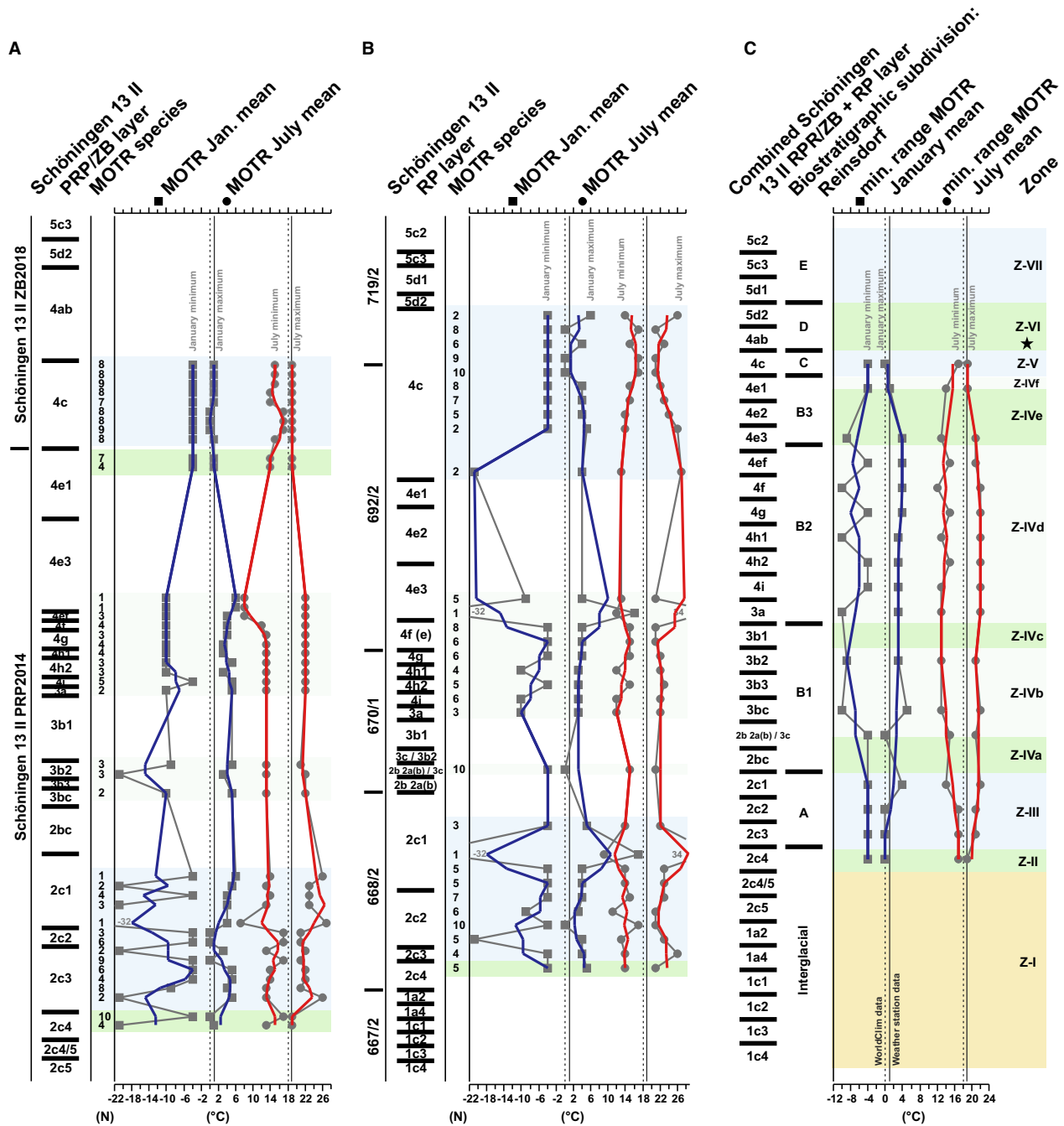


Fig. 3. Reconstructed mean air temperatures ($^{\circ}\text{C}$) for the two sequences: (A) Para-Reference Profile 13 II (2014)/Zeugenblock 13 II (2018) and (B) Reference Profile 13 II (2003) as well as (C) combined minimum ranges of both sequences for all layers of 13 II for January (squares, dark blue curves) and July (circle, red curves) (thicker red and black curves represent the three-point moving averages; vertical line, modern temperatures obtained from local weather stations; vertical dashed line, WorldClim temperature data used for the MOTR calibrations) with number of included species for temperature reconstruction. Black star, position of 'spear horizon'. Colour code and zones corresponding to Fig. 2 (orange, middle- and late-temperate interglacial, thermophile, deciduous-dominated forests; light/dark green, post-temperate interglacial (boreal) forests and post-interglacial woodland and steppe (woodland); blue, post-interglacial steppe (open woodland)).

Zone V (13 II-4c) is marked by the continuous presence of microfossils and the highest ostracod concentrations (up to $787 \text{ valves g}^{-1} \text{ DW}$) and CaCO_3 contents (up to 67%) of the sequence. Comparable with Z-III, *P. zenkeri* (4.9–7.8%) occurs frequently and *P. compressa* is again

almost absent. *Ilyocypris bradyi* and *L. inopinata* are continuously present with increased abundances (6.4–12.2 and 9.7–19.6%, respectively). The diatom assemblage displays a marked shift towards small fragilarioid species (averagely 75.2%), whereas abundances of

benthic taxa decline (on average 23%) compared with those in Z-IVc. The C/N ratios are constantly low (mean, 14). The $\delta^{13}\text{C}_{\text{carb}}$ (−3.2 to −2.6‰) and $\delta^{18}\text{O}_{\text{carb}}$ (−7.6 to −7.3‰) values are stable and generally elevated.

Zone VI extends from sublevel 13 II-4ab to sublevel II-5d2. Diatoms are still present in sublevel 13 II-4ab, although concentrations are decreasing, and ostracods are already absent. The diatom assemblage is still primarily composed of small fragilarioid species (up to 81.1%). The TOC (on average 19%) and C/N ratios (16–18) increase compared with the preceding Z-V.

The uppermost Z-VII (13 II-5c3) is again characterized by the absence of aquatic microfossils. The TOC and C/N ratios are decreasing (minimum values of 1.8 and 11%, respectively).

Mutual Ostracod Temperature Range method

For MOTR reconstructions, 22 species could be used to determine the mutual mean January and July air temperature ranges (Table S1). It is important to understand that the MOTR method only reconstructs ranges of temperatures within which the species of an assemblage could have coexisted, and the actual temperature could have been anywhere within that range. Reconstructed temperature ranges using the MOTR method are often controlled by a few species with very narrow ranges, for example the rare *Fabaeformiscandona balatonica* and *P. zenkeri* (Fig. S2). Nevertheless, all calibrated species in a sample contribute to the reconstruction by confirming mutuality of their temperature ranges, with no outliers. Samples composed of eurythermal species tend to yield a wide temperature range resulting in greater uncertainties. Confidence in the reliability of the method is strengthened by the fact that the MOTR results of both sequences Para-Reference Profile 13 II (2014)/Zeugenblock 13 II (2018) and Reference Profile 13 II (2003) show similar temperature-development trends (Fig. 3).

Reconstructed mean monthly air temperature ranges for the lower part of the sequences (Z-II and Z-III) are often narrow and mainly controlled by the presence of *P. zenkeri*, *Cyclocypris serena*, *I. bradyi*, *Neglecandona altoides*, *Neglecandona lindneri*, *Fabaeformiscandona levanderi*, *Fabaeformiscandona caudata*, and *F. balatonica*. The smallest ranges are −4–0 °C (January) and +17–19 °C (July) in Z-II. Similar mean winter ranges are found in Z-III, whereas the estimated mean July temperature displays a narrow range from +17–21 °C. At the crossover of Z-IVa to Z-IVb mean air temperature ranges remain almost equal (January, −4–0 °C; July, +15–21 °C). We find generally wider ranges (January mean smallest range, −4–3 °C; July mean smallest range, +15–21 °C), between the younger part of Z-IVb up to Z-IVe. These values are mainly constrained by *Candona weltneri*, *N. altoides*, and *I. bradyi* (July) as well as *P. compressa* and *N. altoides* (January). The youngest part of Z-IVe, at the crossover to the overlying Z-

V, exhibits mean January and July air temperature ranges of −4–4 °C and +14–19 °C, respectively. In Z-V, many samples show again a very narrow range of −4–0 °C for January and +17–19 °C for July. Comparable with the lower part of the sequence, *P. zenkeri* and *F. balatonica* are the most important species limiting winter mutual temperature ranges, while mainly *F. balatonica* and *N. lindneri* limit summer ranges.

Comparison of $\delta^{13}\text{C}$ and $\delta^{18}\text{O}$ values between ostracod valves and bulk carbonates

Stratigraphical records of stable oxygen and carbon isotope compositions for bulk carbonates ($\delta^{18}\text{O}_{\text{carb}}$, $\delta^{13}\text{C}_{\text{carb}}$) and ostracod valves ($\delta^{18}\text{O}_{\text{ostracod}}$, $\delta^{13}\text{C}_{\text{ostracod}}$) were obtained for the Reinsdorf sequence from Reference Profile 13 II (2003) (Fig. 4). Ranges of $\delta^{13}\text{C}_{\text{ostracod}}$ in juvenile *Candona* spp. are between −7.5 and 0.8‰. No bulk data are available for Z-II for comparison with the ostracod. Stable oxygen isotope ratios show highly variable values, especially in Z-III, and Z-III also exhibits the largest offsets in $\delta^{18}\text{O}$ between both bulk carbonates and ostracod valves. $\delta^{18}\text{O}_{\text{ostracod}}$ values fluctuate between −9.6 and −5.4‰ with generally lower values in the central part of the sequence (Z-IV). Bulk samples exhibit a generally similar pattern of $\delta^{18}\text{O}_{\text{carb}}$ and $\delta^{13}\text{C}_{\text{carb}}$ with the lowest values mainly in Z-IVd (−9.5 to −8.4‰). However, $\delta^{13}\text{C}_{\text{carb}}$ values are lower and successively increasing throughout Z-II and Z-III (−6.2 to −4.4‰). Zone IV is marked by a positive excursion in both $\delta^{18}\text{O}_{\text{carb}}$ and $\delta^{13}\text{C}_{\text{carb}}$ in sublevel 13 II-4 h.

Zones defined for sequence Para-Reference Profile 13 II (2014)/Zeugenblock 13 II (2018) are clearly distinguished in the $\delta^{13}\text{C}_{\text{carb}}$ and $\delta^{18}\text{O}_{\text{carb}}$ cross-plot and can also be recognized in Reference Profile 13 II (2003) (Fig. 5). More positive $\delta^{18}\text{O}_{\text{carb}}$ values around −8 to −7.5‰ are characteristic for Z-III and Z-V, whereas Z-IV generally exhibits more negative and heterogenous values (−9.5 to −8‰). A further separation of Z-III and Z-V is given by $\delta^{13}\text{C}_{\text{carb}}$, which is around −5.3‰ in the former zone and around −3‰ in the latter. A notable exception is the more negative values at the beginning of Z-V in RP 13 II (2003). The $\delta^{13}\text{C}_{\text{carb}}$ of Z-IV is more variable with values mainly between −6 and −3.5‰.

Discussion

In general, environmental and palaeo-lakeshore changes derived from microfossil assemblages of the Reference Profile 13 II (2003) (Krahn et al. 2021) are confirmed and further refined by the multi-proxy investigations of sequence Para-Reference Profile 13 II (2014)/Zeugenblock 13 II (2018) and complemented for sublevel 13 II-4ab. Our study demonstrates that both the Reinsdorf ostracod fauna and diatom flora responded to and recorded climatic variations with important qualitative

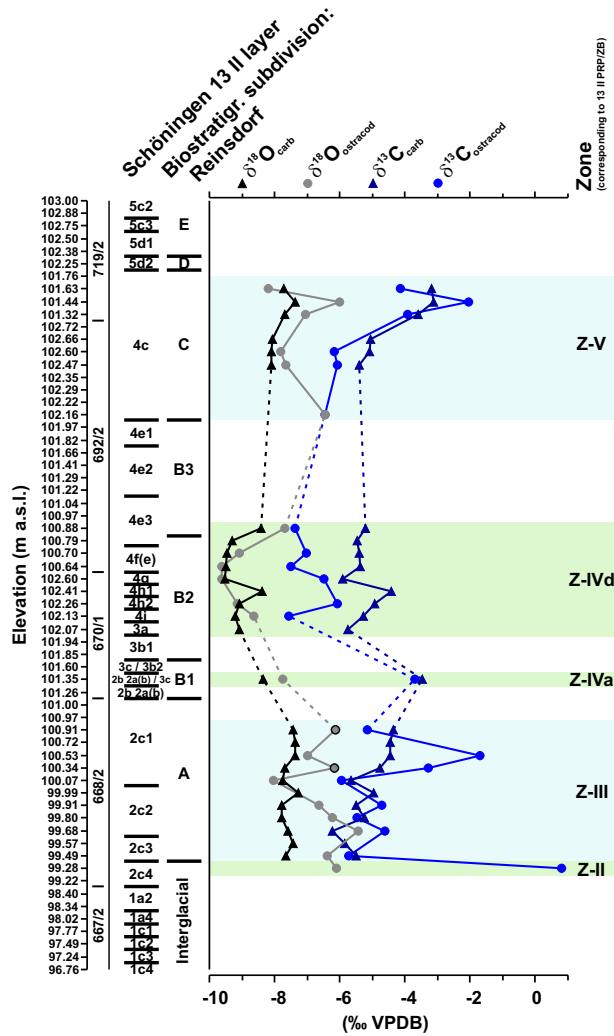


Fig. 4. Stratigraphic diagram of stable oxygen (left, black and grey lines) and carbon isotope ratios (right, blue lines) derived from juvenile *Candona* spp. valves (dot) and bulk carbonates (triangle) from Reference Profile 13 II (2003). Values of $\delta^{18}\text{O}$ and $\delta^{13}\text{C}$ obtained from ostracods are corrected for species-specific vital offsets (+2.2‰ VPDB; von Grafenstein *et al.* 1999). The two black-framed dots in the grey curve indicate samples below the minimum weight limit for detection. Colour code and zones correspond to Fig. 2 (green, post-temperate interglacial (boreal) forests and post-interglacial woodland and steppe (woodland); blue, post-interglacial steppe (open woodland)).

changes in their communities. The new MOTR-based temperature reconstructions and stable isotope analyses facilitate the distinction and characterization of the individual climatic oscillations and effects on the aquatic ecosystem in great detail. The Reinsdorf sequence encompasses a Middle Pleistocene interglacial–glacial transition characterized by changing environments of late-interglacial boreal forests to post-interglacial alternating drier steppe (open woodland) and moister woodland phases, termed the Reinsdorf A–E oscillations (Urban *et al.* 2023a).

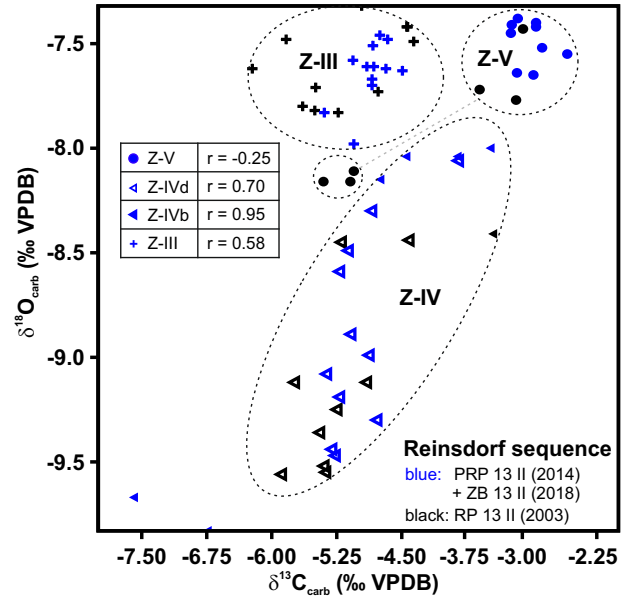


Fig. 5. Bulk carbonate cross-plot of $\delta^{13}\text{C}$ and $\delta^{18}\text{O}$ values from Schöningen sequences Para-Reference Profile 13 II (2014)/Zeugenblock 13 II (2018) and Reference Profile 13 II (2003) with results of correlation analyses of $\delta^{13}\text{C}_{\text{carb}}$ and $\delta^{18}\text{O}_{\text{carb}}$ values in sequence 13 II PRP/ZB. Dashed circles indicate different zones. The two sequences of site 13 II largely overlap regarding values of Z-III–V. In Z-V, the oldest samples of RP 13 II (2003) (three black circles connected by a dashed line to Z-V) are separated from the other samples with values closer to Z-IV of site 13 II.

Interglacial–glacial transitional temperature developments

Reconstructed MOTR temperatures are available starting with the end of Z-II throughout the first post-interglacial steppe (open woodland) phase Reinsdorf A (Z-III; Fig. 3). Mean air temperature estimates following the thermal maximum of the interglacial indicate colder winters as well as summer temperatures within the modern range (January minimum range, -4 – 0 °C, present-day 1 °C weather station data/0 °C WorldClim data; July minimum range, $+17$ – 21 °C (+19 °C in layer II-2c4 based on *F. levanderi*), present-day +18.8 °C weather station data/+18 °C WorldClim data). This is in accord with vegetation changes providing evidence for cooler and dry conditions (Urban & Bigga 2015; Urban *et al.* 2023a), as well as reconstructed temperatures based on plant macro remains. Bigga (2018) calculated for the coldest month in level II-2 minimum temperatures of around -2.5 °C and maximum temperatures of around $+1$ °C. For the warmest month, values ranged from around $+17$ to $+24$ °C. The combination of both methods yields relatively narrow ranges for January and July temperatures of approximately -2.5 – 0 °C and $+17$ – 21 °C (+19 °C with layer II-2c4 of Z-II), respectively. New chironomid-based temperature reconstructions from Schöningen site 13 II suggest summer temperatures to be in the upper range of MOTR reconstructions by

providing evidence for July air temperatures averaging +20 °C during this overall drier phase of Reinsdorf A (Rigterink *et al.* 2024). The apparent consistency between the different proxy-based reconstructions suggests the possibility of deriving Multi-Proxy Consensus ranges (Horne *et al.* 2023) that would be narrower than those obtained from the MOTR method alone, but this will require further checking to ensure stratigraphical equivalence of the different proxy assemblages being compared and is beyond the scope of the present paper.

The MOTR temperature ranges for the following woodland and steppe (woodland) phase (Z-IV, Reinsdorf B) are generally wide and encompass mean temperatures inferred for Z-III, thereby hindering a precise assessment of temperature changes. Combined minimum reconstructed mean air temperature ranges in Z-IV are −4–3 °C for January and +15–21 °C for July (except for the lowermost and uppermost sample) (Fig. 3C). The palynological results hint at rather cool-temperate conditions, thereby suggesting increased temperatures in Z-IV (Urban & Bigga 2015). Chironomid analyses confirm similar or slightly increased summer temperatures compared with those of today (+18–19 °C mean), although not as high as in Z-III (Rigterink *et al.* 2024). Because chironomid reconstructions are restricted to July air temperatures, a reasonable explanation for the overall increased temperatures based on palynological results, despite lower summer temperatures, is higher winter temperatures and thereby a decreased temperature difference between summer and winter (i.e. lower continentality). One exception with lower reconstructed temperatures in the older part of Z-IV is layer 13 II-2b 2a(b)/3c. Here, in particular, mean winter air temperatures are comparable with Z-III with mutual ranges of −4–0 °C, based on the occurrence of *F. balatonica*, which hints at a short climatic oscillation with cooler temperatures during this woodland-steppe phase.

The closest mutual ranges of the two site 13 II sequences indicate mean air temperature ranges of −4–0 °C in January and +17–19 °C in July for Z-V (Reinsdorf C), which is almost identical to temperatures inferred for Z-III (Fig. 3C). The temperatures during this climatic oscillation seem to have been in the same range as present-day summers, while the winters were at least 1 °C colder (or similar compared with the WorldClim data), suggesting a more continental climate compared with Z-IV. Low winter temperatures are also in accordance with prolonged lake ice cover suggested by high abundances of small fragilarioid diatoms (Lotter & Bigler 2000), and the cool, dry conditions during the development of a grass-rich steppe ecosystem (Urban & Bigga 2015) (Fig. 2). Chironomid-based summer temperature reconstructions during this late phase of the Reinsdorf sequence were hindered by decreased species richness and the dominance of a certain chironomid taxa which lead to an overestimation of temperatures (Rigterink *et al.* 2024).

Lakeshore and catchment dynamics throughout the Reinsdorf sequence

Seven main zones (Z-I–VII) were defined in the sequence based on changes in biological and geochemical proxies and the established biostratigraphic subdivision (Reinsdorf A–E; Fig. 2, Table 1). Three distinct environmental oscillations, represented by both microfossil and bulk stable isotope data, were herein recognized, partly interrupted by periods of poor preservation and lack of remains and isotope data. These environmental phases are characterized by (i) Reinsdorf A – *P. zenkeri*–*I. bradyi*, no diatoms, medium $\delta^{13}\text{C}_{\text{carb}}$ and higher $\delta^{18}\text{O}_{\text{carb}}$ (Z-III); (ii) Reinsdorf B – *P. compressa*, increased abundances of benthic diatoms, variable $\delta^{13}\text{C}_{\text{carb}}$ and lower $\delta^{18}\text{O}_{\text{carb}}$ (Z-IV); and (iii) Reinsdorf C – *P. zenkeri*–*I. bradyi*–*L. inopinata*, dominance of small fragilarioid diatoms, higher $\delta^{13}\text{C}_{\text{carb}}$ and higher $\delta^{18}\text{O}_{\text{carb}}$ (Z-V) (Fig. 2).

In lake systems, stratigraphical changes in $\delta^{18}\text{O}$ values are often attributed to changes in temperature, seasonality, hydrology and the precipitation/evaporation (P/E) balance (Leng & Marshall 2004). Lower temperatures result in more negative $\delta^{18}\text{O}$ of precipitation, while concurrently temperature-dependent fractionation during carbonate formation in the water leads to enriched bulk carbonate $\delta^{18}\text{O}$ values at lower temperatures. Especially in closed lakes, increased evaporation leads to a preferential loss of ^{16}O to the atmosphere and thereby ^{18}O -enriched lake water (Teranes & McKenzie 2001; Leng & Marshall 2004; Xu *et al.* 2006). Changes in the catchment hydrology, such as increased input of isotopically enriched detrital carbonates through rivers and streams into the lake, could also lead to more positive $\delta^{18}\text{O}$ values (Hammarlund & Buchardt 1996). Lacustrine carbonate $\delta^{13}\text{C}$ values can be influenced by parameters such as algal productivity, the degradation of organic matter, water residence time, vegetation changes within the catchment, river or groundwater discharge into the lake and CO_2 exchange with the atmosphere (Schelske & Hodell 1991; Aravena *et al.* 1992; McKenzie & Hollander 1993; Leng & Marshall 2004; Lu *et al.* 2010). Preferential assimilation of lighter ^{12}C by phytoplankton during photosynthesis results in the enrichment of ^{13}C and more positive $\delta^{13}\text{C}$ values of carbonates forming in the surface waters, whereas oxidation during the decay of organic matter at the lake bottom may release ^{12}C -enriched CO_2 and decrease $\delta^{13}\text{C}_{\text{carb}}$ values (Schelske & Hodell 1991; Schwab 2003). Higher $\delta^{13}\text{C}_{\text{carb}}$ values may correspond to a development of a poorly vegetated or C_4 plant-dominated vegetation cover within the catchment or vice versa (Andrews *et al.* 1997; Hammarlund *et al.* 1997; Liu *et al.* 2019). High $\delta^{13}\text{C}_{\text{carb}}$ can also be produced by the dissolution of old carbonate catchment rocks or detrital carbonate input (Hammarlund & Buchardt 1996; Leng & Marshall 2004; Leng *et al.* 2010; Mangili *et al.* 2010). We generally interpret more negative bulk carbonate $\delta^{18}\text{O}$

values in our record to correspond to overall wetter conditions and cooler summer temperatures, resulting in increased freshwater discharge into the lake and a decreased P/E balance as well as more negative $\delta^{18}\text{O}$ precipitation values. More negative bulk carbonate $\delta^{13}\text{C}$ values are mainly attributed to tree cover expansion and reduced photosynthetic activity. However, the signals are influenced by a wide range of interlinked processes and the effects might dampen or amplify each other. The following subsections related to Reinsdorf A, Reinsdorf B and Reinsdorf C describe in detail changes in lakeshore and catchment dynamics based on changes in the biological and geochemical proxies.

Terminating Reinsdorf Interglacial (Z-I–Z-II) and first post-interglacial steppe (open woodland) phase (Z-III, Reinsdorf A). – The interglacial temperature maximum and its terminal phase in the beginning of sequence PRP 13 II (2014)/ZB 13 II (2018) (Z-I/Z-II) are not recorded in the microfossil record, probably because of very low lake levels and/or poor preservation of remains (Fig. 2). The C/N ratios of the following Z-III are in the lower range of the record at about 13–18, thereby suggesting higher proportions of aquatic-derived organic matter and increased lake levels (Meyers 1994; Brodie *et al.* 2011).

The first steppe (open woodland) phase Reinsdorf A (Z-III) is represented by *P. zenkeri*–*I. bradyi*, no diatoms, medium $\delta^{13}\text{C}_{\text{carb}}$ and higher $\delta^{18}\text{O}_{\text{carb}}$ (Figs 2, 5). It must be noted, however, that diatoms, mainly small fragilaroid species, were present in sub-sublevel II-2c1 of RP 13 II (2003) (Krahn *et al.* 2021). Their lack in this part of the PRP 13 II (2014) can probably be attributed to preservation effects. The ostracod *P. zenkeri* avoids standing and deep waters, preferring slow-flowing, vegetated streams, and is often associated with groundwater issues (spring flows), and *I. bradyi* is considered to be mesorheophilic (Meisch 2000). The co-occurrence of both species and the low MOTR reconstructed mean winter air temperatures (Fig. 3) probably suggest an increased influence of flowing waters, probably from surface stream inflow at the lakeshore originating from springs at the Elm ridge during a phase with colder winters. Our new results thereby confirm previous microfossil- and pollen-based interpretations pointing towards a seasonally cooler and drier climate oscillation with reduced vegetation cover resulting in increased surface runoff in the catchment (Urban & Bigga 2015; Krahn *et al.* 2021; Tucci *et al.* 2021; Urban *et al.* 2023a), and additionally provide quantitative temperature data. The climate could have been more continental (Fig. 6A), as suggested by Urban and Bigga (2015) based on vegetational data, with increased seasonal temperature variations (colder winters and warmer summers) and overall reduced annual precipitation (Duckson 1987). The higher water table in Z-III compared with the interglacial temperature maximum as suggested by the presence of aquatic microfossils and a generally

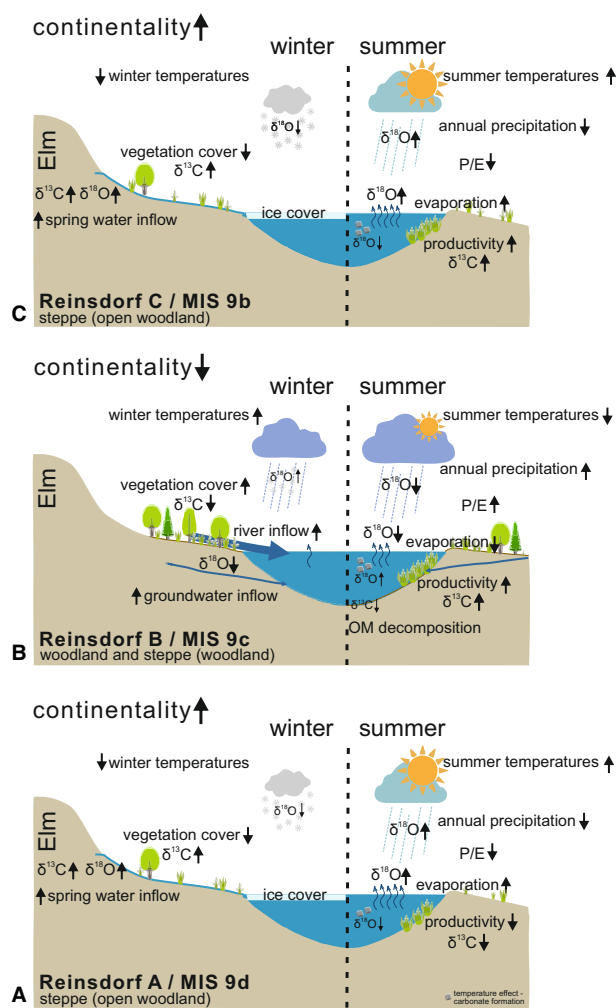


Fig. 6. Schematic visualization of the three most characteristic climatic oscillations (A–C) following the temperature maximum of the Reinsdorf interglacial with important processes influencing the isotopic composition of carbonates. The chronological allocations given represent scenario 1, which is considered more plausible. The allocations of scenario 2 can be found in Table 1.

lower C/N ratio (see also Urban *et al.* 2023a), despite drier conditions, is most probably a consequence of decreased vegetation cover and loss of woodland (Fig. 2), leading to reduced transpiration (Behre *et al.* 2005; Urban *et al.* 2023a). Alternatively, a decrease in lake evaporation as a consequence of overall cooler temperatures could have led to a higher water table as well. A peak in $\delta^{13}\text{C}_{\text{ostracod}}$ can be observed in the upper part of Z-III and might be the effect of moulting of the *Candona* valves during the colder season (Leng & Marshall 2004). The silty sands of the uppermost part of Z-III are void of ostracods, which is probably related to a depositional event at the transition to the succeeding layer as proposed by Urban *et al.* (2023a).

First post-interglacial woodland and steppe (woodland) phase (Z-IV, Reinsdorf B). – Progressive lake level

lowering at the beginning of the woodland and steppe (woodland) phase (Z-IVa, Reinsdorf B1) probably led to an increased influence of terrestrially derived organic matter, visible in rising C/N ratios (up to 23) and the highest TOC contents (Fig. 2).

Ostracods reappear in Z-IVb confirming at least temporary submerged conditions with sufficient oxygen availability. Concentrations, however, are low and many valves were found broken and could only be identified to genus level. Their poor preservation is probably attributable to still increased contents in organic matter (Fig. 2) and associated bacterial activity, resulting in lower pH and dissolution of the calcareous valves (De Deckker 2002).

A significant environmental shift is detected at the top of Z-IVb, as documented by an initial marked decrease in $\delta^{13}\text{C}_{\text{carb}}$ and $\delta^{18}\text{O}_{\text{carb}}$ records and generally lower values in $\delta^{18}\text{O}_{\text{carb}}$ in Z-IV (Figs 2, 4, 5). The sediment type changes from an organic mud to a silicious and subsequently calcareous mud (Fig. 2). The $\delta^{18}\text{O}_{\text{carb}}$ and $\delta^{18}\text{O}_{\text{ostracod}}$ values are relatively similar with just slightly higher values in the ostracod record (Fig. 4), hinting at a shallow, well-mixed lake without much difference between bottom waters (ostracods) and surface waters (authigenic carbonates, bulk) (Schwalb 2003). We therefore assume that the input of detrital carbonate was minor. Reduced evaporation with concurrently increased less-evaporative enriched river inflow would result in lower $\delta^{18}\text{O}_{\text{carb}}$ values. Therefore, we propose that a wetter, less continental climate with a changed P/E balance towards increased precipitation has led to the more negative $\delta^{18}\text{O}_{\text{carb}}$ values during this woodland and steppe (woodland) phase (Fig. 6B). Today, precipitation in the region is highest during the summer months (IAEA/WMO 2022) and lower summer temperatures, leading to overall lower $\delta^{18}\text{O}$ values of the annual precipitation signal, would have contributed to lower $\delta^{18}\text{O}$ values of the lake water as well (Schwalb 2003; Leng & Marshall 2004). Comparable $\delta^{13}\text{C}_{\text{carb}}$ values of Z-III and Z-IV are probably the result of two opposing effects: (i) decreasing $\delta^{13}\text{C}_{\text{carb}}$ because of a denser vegetated catchment together with possibly less influence of spring waters more strongly influenced by dissolved old carbonates from the limestone ridge (Hammarlund & Buchardt 1996; Leng & Marshall 2004; Leng et al. 2010; Mangili et al. 2010), as suggested by the disappearance of the ostracod *P. zenkeri* in Z-IV, with concurrently (ii) increasing $\delta^{13}\text{C}_{\text{carb}}$ owing to enhanced photosynthetic productivity, as inferred from the aquatic fauna and flora and higher organic matter contents (Böhme 2015; Krahn et al. 2021; Figs 2, 5), leading to a ^{12}C depletion in the dissolved inorganic carbon pool and consequently ^{13}C enrichment in authigenic carbonates forming in surface waters (Schwalb 2003; Leng & Marshall 2004).

The appearance of diatoms in PRP 13 II (2014) as well as the lack of ostracods, low CaCO_3 , further decreasing TOC and variable C/N with generally elevated values characterize sub-sublevel 13 II-3b1 (Z-IVc, Fig. 2),

suggesting reduced aquatic productivity and/or anoxic bottom conditions. The latter is also supported by low Fe/Ti ratios, indicating increasing anoxia (Urban et al. 2023a). The absence of diatoms that usually occur in almost all types of habitats (Battarbee et al. 2001) in the older sections of the sequence (Z-I–IVb) is probably related to unfavourable preservation conditions (Flower 1993).

Significantly increased abundances of *P. compressa* in Z-IVd (Reinsdorf B2; Fig. 2), with concurrent decreases in the prominent, flowing waters indicating species of Z-III, indicate a change towards calmer environmental conditions close to the lakeshore at site 13 II. *Pseudocandona compressa* is considered to be oligorheophilic, mesothermophilic and oligo- to mesohalophilic, and generally occurs in shallow areas of both temporary and permanent water bodies (Meisch 2000). A stream flows nowadays from the north towards the study area (Missaue, Fig. 1B). The well-vegetated catchment during this phase probably reduced the direct inflow of the smaller, eastwards-located spring streams at site 13 II during deposition of Z-IV sediments, and the lake water could have been more strongly influenced by increased ‘pre-Missaue’ river and groundwater discharge as suggested by lower $\delta^{18}\text{O}_{\text{carb}}$ values (Fig. 6B). Krahn et al. (2021) reconstructed higher salinities for this phase and proposed increased groundwater input, influenced by the nearby salt wall. Common epiphytic diatom species occurrences (e.g. *Cocconeis* spp.; Fig. S1) hint at rich aquatic vegetation. Although decreasing towards the top of Z-IV, overall elevated C/N ratios suggest an increased influence of terrestrial organic matter and lower lake levels (Fig. 2). Interestingly, palynological findings characterize the Reinsdorf B2 oscillation as a cooler and drier period within the first post-interglacial woodland phase Reinsdorf B with shallowing lake levels and increased seasonality (Urban et al. 2023a). This period seems to have been especially favourable for microfossil development and/or preservation at the study site. More negative $\delta^{13}\text{C}_{\text{ostracod}}$ in comparison with the bulk data (Fig. 4) can be explained by ^{12}C -enriched bottom waters from decomposition of organic matter (Fig. 6B). Parallel trends of $\delta^{13}\text{C}_{\text{carb}}$ and $\delta^{18}\text{O}_{\text{carb}}$ are interpreted to reflect variable stream input in a closed lake system in Z-IV (Figs 2, 5).

Both sequences from site 13 II, RPR 13 II (2014)/ZB 13 II (2018) and RP 13 II (2003), document a sudden shift towards higher $\delta^{18}\text{O}_{\text{carb}}$, $\delta^{13}\text{C}_{\text{carb}}$, TOC and C/N values around sub-sublevel II-4 h1 and II-4 g (Figs 2, 4). Additionally, reduced microfossil abundances and partly changed species assemblages, such as the short appearance of the ostracod *L. inopinata*, are visible in both records (Krahn et al. 2021; this study). Krahn et al. (2021) interpreted this prominent change in RP 13 II (2003) as a local erosion event caused by dry–wet oscillations. However, because the signal can be observed in both

sequences, we hypothesize a short-lived climatic oscillation causing lake-level fluctuations.

To sum up, the woodland and steppe (woodland) phase Reinsdorf B2 (Z-IV), characterized by *P. compressa* – increased abundances of benthic diatoms – variable $\delta^{13}\text{C}_{\text{carb}}$ and lower $\delta^{18}\text{O}_{\text{carb}}$, probably reflects a period with a higher P/E balance with increased freshwater input and reduced annual temperature variations compared with Z-III (Fig. 6B). A denser vegetation cover with an increased percentage of trees and shrubs in the catchment (Fig. 2) during most parts of this phase may have resulted in higher infiltration rates promoting enhanced groundwater and river discharge into the lake at the expense of smaller Elm spring inflows at the lakeshore, leading to calmer lake conditions, while productivity was generally increased.

In the following Z-IVe (Reinsdorf B3), C/N ratios decrease (minimum 13) and imply an enhanced influence of algae-derived organic matter because of further increased lake levels (Fig. 2). However, both ostracods and diatoms disappear completely and falling lake levels with enhanced input of soil organic matter from C_3 -plants with low C/N ratios (Talbot 2001; Enters *et al.* 2006; Sanderman *et al.* 2015) could also be plausible. Urban *et al.* (2023a) propose an increased lake level based on lake-floor anoxia, a shift towards generally more aquatic but simultaneously reduced bio-productivity and enhanced minerogenic input. Rigterink *et al.* (2024) also concluded rising lake levels based on decreasing abundances of littoral chironomid taxa. The barren microfossil samples are therefore probably the result of both anoxia and preservation effects.

In the uppermost part of sub-sublevel Z-IVf at the transition into Z-V ostracods are again present and minerogenic input is reduced (Urban *et al.* 2023a), suggesting more oxygenated conditions and increasing bio-productivity; the reappearance of *P. zenkeri* suggests a return to higher spring-fed stream flow.

Second post-interglacial steppe (open woodland) phase (Z-V, Reinsdorf C). – A permanent lake with probably higher levels existed throughout Z-V, as documented by frequent occurrences of ostracods and diatoms and low C/N ratios as well as high CaCO_3 contents (Fig. 2). The combination *P. zenkeri*–*I. bradyi*–*L. inopinata* – dominance of small fragilarioid diatoms – higher $\delta^{13}\text{C}_{\text{carb}}$ and higher $\delta^{18}\text{O}_{\text{carb}}$ (Figs 2, 5) is characteristic for the steppe (open woodland) phase Reinsdorf C. Notably decreased numbers of the ostracod *P. compressa*, characteristic for Z-IV and interpreted to represent calmer conditions, in favour of ostracod species preferring flowing waters (e.g. *P. zenkeri*) suggest a return to conditions more comparable with Z-III with increased inflows of surface streams at the study site. Similar $\delta^{13}\text{C}$ and $\delta^{18}\text{O}$ values for both bulk carbonates and ostracods (Fig. 4) suggest a well-mixed water column (Schwalb 2003). The prominent small fragilarioid diatoms are often considered

opportunistic pioneer species because of their fast reproduction rate and wide tolerance for most environmental parameters, which makes them highly competitive in unstable, changing habitats (Hickman & Reasoner 1994, 1998; Lotter & Bigler 2000; Weckström & Juggins 2005). Their mass development is proposed to be stimulated by environmental instability (Denys 1990) and high abundances in late glacial and early postglacial lake records (Haworth 1976; Smol 1983) were associated with long periods of ice cover on the lake (Lotter & Bigler 2000). The common *L. inopinata* mainly occurs in the littoral zone and is considered to be tolerant to a wide range of environmental conditions, especially high alkalinity (Löffler 1959; Meisch 2000). Its higher abundance compared with Z-III suggests increased alkalinity of lake water in Z-V, possibly connected to high aquatic productivity, which was concluded from chironomid data for this phase (Rigterink *et al.* 2024).

Concomitant shifts in both $\delta^{13}\text{C}$ and $\delta^{18}\text{O}$ values generally hint at changes in hydrology (Schwalb 2003). Both $\delta^{13}\text{C}$ and $\delta^{18}\text{O}$ in bulk carbonate and ostracod records document a change to more positive values in Z-V (Fig. 4), probably attributable to a stronger effect of a more continental climate with a lower P/E balance and decreased ‘pre-Missaue’ river discharge into the lake with a higher contribution of spring water surface discharge, isotopically enriched by evaporation and possibly enriched in bicarbonate from the Elm limestone ridge (Figs 1B, 6C). Increased annual temperature variations with higher $\delta^{18}\text{O}$ in summer precipitation would also have contributed to more positive isotope signals. Significantly higher numbers of aquatic microfossil remains indicate that the more positive $\delta^{13}\text{C}_{\text{carb}}$ in Z-V compared with Z-III could be ascribed to higher bio-productivity and increased preferential assimilation of lighter ^{12}C during photosynthesis (Andrews *et al.* 1997; Hammarlund *et al.* 1997; Schwalb 2003; Liu *et al.* 2019), possibly as a result of increased erosion and nutrient input connected to a reduced vegetation cover. Furthermore, higher abundances of calcareous charophyte remains in the Characeae rich silt of layer II-4c (Urban *et al.* 2023a) could also have produced higher $\delta^{13}\text{C}_{\text{carb}}$ values (Ito 2001).

Final transition of the Reinsdorf sequence (Z-VI–Z-VII, Reinsdorf DIE). – Organic-rich deposits may have led again to the dissolution of ostracod valves during Reinsdorf D, while siliceous diatoms are still present in progressively decreasing abundances (Fig. 2). This suggests at least temporary water coverage of the lakeshore site, although lake levels may have been low for much of the time. Despite the reconstructed return to a forest-steppe vegetation (Urban *et al.* 2023a), dominant small fragilarioid diatom taxa still suggest habitat instability and periods of extended ice cover at the lake, pointing to cooler winter temperatures during Reinsdorf D. Sublevel 13 II-4ab represents the famous ‘spear

horizon' and findings support human hunting in wet mud (Musil 2007; Voormolen 2008) or on temporary exposed plains (Lang *et al.* 2012, 2015), rather than on dried lakeshore sites (Thieme 2007). Our results are also in accordance with interpretations based on combined biological, lithological and geochemical analyses (Stahlschmidt *et al.* 2015; Urban & Bigga 2015) pointing to submerged conditions. However, investigations of several short sediment sections covering the spear horizon and the underlying sublevel II-4c, distributed along the palaeo-lakeshore, hint at a diverse pattern with varying degrees of microfossil preservation (Urban *et al.* 2023b). Decreasing lake levels and progressive silting up are also suggested by rising C/N ratios and high TOC, comparable with Z-IVa. Overall dominance of small tychoplanktonic diatoms (Fig. 2) suggests unstable aquatic habitats and/or prolonged ice cover on the lake during winter.

The top of the sequence (Reinsdorf E; Fig. 2) is marked by a severe environmental change leading to a lack of aquatic microfossils, while most geochemical parameters exhibit a drop (TOC, C/N). We attribute these shifts to a further lake-level drop. Soil organic matter from C₃-plants can also have low C/N ratios close to the range of freshwater algae (Talbot 2001; Enters *et al.* 2006; Sanderman *et al.* 2015), and lower C/N ratios might be the result of decreasing vegetation cover at the transition towards a more steppe-like environment with increased erosion of soil organic matter into the lake.

Chronological position of the Reinsdorf climate oscillations

Luminescence dating of the Reinsdorf sequence (Reinsdorf A, level 13 II-2c1) gives an age of around 300 ka (Tucci *et al.* 2021), thereby suggesting an allocation of the interglacial part of the sequence to the MIS 9 climatic optimum (e.g. Railsback *et al.* 2015). However, in the absence of an absolute chronology, it remains unclear which timespan the Reinsdorf sequence covers and, consequently, if the full transition into the next glacial stage (i.e. MIS 8) is documented in our record. On this basis, we propose two alternative stratigraphic positions for the Reinsdorf sequence (scenarios 1 and 2, Table 1).

In the first scenario, the interglacial forest phase (Urban *et al.* 2023a) could be correlated with substage MIS 9e (e.g. Desprat *et al.* 2009; Sadori *et al.* 2016; Koutsodendrīs *et al.* 2023). Given that stadial intervals of the Middle–Late Pleistocene interglacials across Europe are marked by the expansion of steppe biomes (Reille *et al.* 2000; Sadori *et al.* 2016; Koutsodendrīs *et al.* 2023), the two cool steppe (open woodland) phases Reinsdorf A and Reinsdorf C that follow the interglacial forest phase can be correlated to the MIS 9d and MIS 9b stadials, respectively (Table 1). Accordingly, the interjacent woodland phase Reinsdorf B could be correlated to MIS 9c, whereas the second woodland phase Reinsdorf

D could be correlated to MIS 9a. The top of the Reinsdorf sequence, which is characterized by a post-interglacial steppe-tundra phase (Reinsdorf E), could be subsequently correlated to MIS 8c.

In the second scenario, the cooler steppe phases Reinsdorf A and C could alternatively represent suborbital cold events within MIS 9d as they have been documented in records from the Iberian margin (Roucoux *et al.* 2006; Martrat *et al.* 2007; Desprat *et al.* 2009). Specifically, the integration of palynological and sea-surface temperature records off Iberia suggests that two forest contractions (3NWI-fr2 and -fr3) directly correspond to two cooling events (3IMS-15 and -14) during MIS 9d (Desprat *et al.* 2009). These climatic oscillations have been linked to changes in the deep-water circulation of the North Atlantic and possibly an amplification of the reduction in Atlantic Meridional Overturning Circulation by iceberg discharges. Such climate change could also have affected vegetation in the central European lowlands (Sirocko *et al.* 2005; Kern *et al.* 2022), hence suggesting a potential correlation of the Reinsdorf A and C steppe phases to the 3NWI-fr2 and -fr3 events from the Iberian margin records, and by extension the Reinsdorf E phase to MIS 9c.

While both stratigraphical scenarios are possible, a close inspection of the palynological data from the Reinsdorf sequence suggests the first one as more probable. Specifically, the woodland phase Reinsdorf B is subdivided into three phases (Reinsdorf B1–B3), with the sub-phase Reinsdorf B2 representing an interjacent cool and dry phase (Urban *et al.* 2023a). Assuming a correlation of the Reinsdorf B with MIS 9c, the B2 sub-phase may correspond to the forest contraction 3NWI-fr6 and stadial 3IMS-12 that have been documented during MIS 9c (at *c.* 307 ka) in records from the Iberian margin (Desprat *et al.* 2009). This event is also documented in several other European records. In a pollen record from the French Massif Central, the Ussel interstadial, a moderate temperate and fairly long period corresponding to MIS 9c, is interrupted by an abrupt cold fluctuation (labelled PraC 37), associated with the expansion of steppe taxa (Reille *et al.* 2000). Moreover, the Tenaghi Philippon record from SE Europe shows two forest expansion events (labelled A1 and A2) during MIS 9c, intersected by a reduction of arboreal and temperate pollen percentages at *c.* 309 ka (Fletcher *et al.* 2013; Koutsodendrīs *et al.* 2023). Independent evidence for climate variability during MIS 9c is further provided by a speleothem record from SE Europe, documenting the interruption of a generally wet climate by a marked event of reduced precipitation at around 310 ka (Regattieri *et al.* 2018). If Reinsdorf B2 corresponds to this mid-MIS 9c oscillation documented across southern Europe from Iberia to the Balkan Peninsula, however, the two aforementioned cold events during MIS 9d (3NWI-fr2 and -fr3, 3IMS-15 and -14) would not have a representation in the Reinsdorf sequence. This can possibly be

explained by a weaker imprint of these events on the central European vegetation under stadial cool and dry conditions. Finally, the treeless steppe-tundra vegetation (Reinsdorf E) at the top of the Reinsdorf sequence (Urban *et al.* 2023a) is associated with the first weakly developed frost structures, such as ice-wedge fissures and cryoturbations (level II-5, Mania & Altermann 2015), typical for a periglacial environment (Urban 2007). The cold and dry conditions derived from these findings thus strongly support the interpretation of a transition into the next glacial stage (MIS 8), hence making the first scenario for the stratigraphical position of the Reinsdorf climate oscillations within the marine isotope stratigraphy more plausible.

Temperature comparison of the Reinsdorf sequence with other Middle Pleistocene records

European MOTR data of MIS 9 for comparison is scarce, especially for the post-interglacial phases. MIS 9 interglacial MOTR reconstructions from Purfleet, UK, encompass January mean air temperature ranges of -3 – 3 °C and July ranges of $+16$ – 21 °C, which is consistent with other British records and proxies (Bridgland *et al.* 2013). Compiled MOTR results for other UK MIS 9 sites produce even narrower consensus ranges with winter temperatures of -3 – 1 °C and summer temperatures of $+16$ – 19 °C. These July temperatures are consistent with the modern UK range but allow the possibility that summers were one or two degrees warmer, while winter temperatures were colder. However, a comparison of these data with the Reinsdorf sequence is problematic because the British records mainly cover the warmest substage (MIS 9e), and it cannot be determined if stratigraphically younger deposits represent this same substage or one of the later substages of MIS 9. In contrast to the British records, MOTR data from Schöningen are only available for the interglacial–glacial transition following the temperature maximum.

It has long been discussed whether the Reinsdorf represents a regional variety of the Holsteinian and if the Holsteinian corresponds to MIS 11 or 9 (see above). Therefore, a comparison of the Reinsdorf data with available European Holsteinian and Hoxnian (MIS 11) data is presented in this paragraph. Holsteinian Interglacial MOTR-based temperature reconstructions from Bilzingsleben (Germany) show mean January air temperatures of -4 – 4 °C and mean July air temperatures of $+16$ – 20 °C, indicating mild winter and summer temperatures similar to the present-day climate (Daniel & Frenzel 2023). Multiproxy temperature reconstructions from Hoxne (UK) suggest similar or around 3 °C cooler winter temperatures and similar or up to 4 °C higher summer temperatures during the Hoxnian interglacial period which is correlated to MIS 11c (Horne *et al.* 2023). In a succeeding cold interval, a multi-proxy consensus using ostracods, beetles, chironomids and plant macrofossils

showed that temperatures were reduced by around 3–5 and 2.5 °C compared with present-day during winter and summer, respectively (mean January -2 – 0 °C), although it must be noted that the mutual overlap of the MOTR and Beetle Mutual Climatic Range methods alone showed much colder winters at Hoxne, at least 5 °C cooler than in the present day (Horne *et al.* 2023). The application of the MOTR method at another UK MIS 11 site, West Stow, has shown a post-interglacial cold interval with mean January temperatures of -1 °C or lower (Benard-out 2015). The reconstructions for the post-interglacial phases of these two MIS 11 sites in the UK indicate greater summer and winter cooling during the cold interval compared with our results, which, apart from the palynological differences of Holsteinian sequences, further supports the assignment to two different MIS and consequently the present correlation of the Reinsdorf sequence to MIS 9 instead of MIS 11.

Conclusions

The full interglacial phase, which possibly corresponds to MIS 9e based on luminescence dating results, and its transition into a first cooler phase (Z-I and Z-II), the Reinsdorf A oscillation, were marked by low lake levels, probably connected to increased evapotranspiration. Lower P/E balance, reduced vegetation cover, landscape instability and erosion with pronounced streams fed by springs from the Elm mountain ridge during periods of greater continentality are depicted for Reinsdorf oscillations A and C (Z-III and Z-V), which probably represent MIS 9d and MIS 9b, respectively. Winter temperatures were lower (narrowest January range, -4 – 0 °C) compared with today and summer temperatures embraced present-day values (narrowest July ranges, $+17$ – 19 or $+17$ – 21 °C). The interjacent Reinsdorf B period (Z-IV) is characterized by a more humid climate with denser vegetation cover in the catchment, associated with increased river and groundwater discharge and temporarily more stable aquatic habitats and higher lake levels at the study site. A dynamic lake system with fluctuating lake levels is depicted by highly variable geochemical parameters and microfossil abundances for this period, which was tentatively correlated to MIS 9c. Reconstructed monthly mean air temperatures yield wide ranges, especially for January (-4 – 3 °C). The famous ‘spear horizon’ (Z-VI) of the Reinsdorf D is marked by another phase of decreasing lake levels during an open woodland environment and might correspond to MIS 9a. Still submerged conditions or at least temporary water coverage are followed by a further lake level drop in the uppermost part of the sequence (Z-VII), which is already characterized by a steppe-tundra vegetation at the onset of phase Reinsdorf E (probably MIS 8c).

In the absence of an absolute chronology, a second chronological position of the Reinsdorf sequence was proposed in addition to the aforementioned allocations

of the phases Reinsdorf A–E to MIS 9d–8c, respectively. In this alternative scenario, the two cool steppe phases Reinsdorf A and C would correspond to suborbital North Atlantic cooling episodes punctuating MIS 9d (3IMS-15 and -14), and the Reinsdorf sequence would consequently end within substage MIS 9c. However, considering the pronounced interjacent cool and dry phase during the first woodland phase (Reinsdorf B), comparable with findings in other European records during MIS 9c, and the cold, rather periglacial conditions derived for the top of the Reinsdorf sequence (Reinsdorf E, level 13 II-5), the first scenario appears at present more plausible.

Investigation of two lakeshore sequences and multiple proxies from Schöningen helps to overcome limitations posed by depositional gaps in the individual sequences and varying preservation of microfossils, and to further distinguish between sequence-specific and climate signals. The new qualitative and quantitative multi-proxy investigations from the Reinsdorf sequence of Schöningen provide evidence for considerable climate variability during the interglacial–glacial transition of MIS 9. Our study contributes to the understanding of younger Middle Pleistocene climate dynamics as well as aquatic ecosystem responses to the MIS 9 environmental oscillations. Furthermore, our research presents one of the first more detailed, quantitative MIS 9 temperature reconstructions for central Europe.

Acknowledgements. – This study is a contribution to the project ‘Climate and Environmental Variability during the late Middle Pleistocene at the Paleolithic Sites of Schöningen, Northern Germany’, funded by Deutsche Forschungsgemeinschaft (DFG grant SCHW 671/22-1, UR 25/11-1; project number 350769604). We wish to thank N. Conard, S. Gaudzinski-Windheuser, V. Mosbrugger, T. Terberger, E. Turner and T. van Kolfschoten, for supporting the project. The authors wish to thank J. Serangeli and the excavation team. We thank B. Schröder for her helpful advice on the stable isotope data. Peter Frenzel is gratefully acknowledged for his help in ostracod identification. We are thankful to the student assistants who helped with the laboratory work. Jan A. Piotrowski is acknowledged for editorial handling and Leszek Marks is acknowledged for guest-editorial handling. Thijs van Kolfschoten and an anonymous reviewer provided constructive comments on an earlier version of the manuscript. Open Access funding enabled and organized by Projekt DEAL.

Author contributions. – AS and BU designed the project and acquired funding. BU and MT provided the sample material. KJK performed part of the aquatic microfossil laboratory work and analyses, conducted data processing and overall multi-proxy data interpretation, and provided the figures. DJH provided the MOTR calibrations. SP performed the element and stable isotope analyses. AK cooperated on this project. KJK wrote the text with the contributions from all authors. All co-authors contributed to the manuscript by proofreading and discussions.

Data availability statement. – The data that support the findings of this study are available from the corresponding author upon reasonable request.

References

Andrews, J. E., Riding, R. & Dennis, P. F. 1997: The stable isotope record of environmental and climatic signals in modern terrestrial

- microbial carbonates from Europe. *Palaeogeography, Palaeoclimatology, Palaeoecology* 129, 171–189.
- Aravena, R., Warner, B. G., MacDonald, G. M. & Hanf, K. I. 1992: Carbon isotope composition of lake sediments in relation to lake productivity and radiocarbon dating. *Quaternary Research* 37, 33–345.
- Battarbee, R. W. & Kneen, M. J. 1982: The use of electronically counted microspheres in absolute diatom analysis. *Limnology and Oceanography* 27, 184–188.
- Battarbee, R. W., Jones, V. J., Flower, R. J., Cameron, N. G., Bennion, H., Carvalho, L. & Juggins, S. 2001: Diatoms. In Smol, J. P., Birks, H. J. B. & Last, W. M. (eds.): *Tracking Environmental Change Using Lake Sediments. Volume 3: Terrestrial, Algal, and Siliceous Indicators*, 155–202. Kluwer Academic Publishers, Dordrecht.
- Behre, K.-E., Hölzer, A. & Lemdahl, G. 2005: Botanical macro-remains and insects from the Eemian and Weichselian site of Oerel (northwest Germany) and their evidence for the history of climate. *Vegetation History and Archaeobotany* 14, 31–53.
- Benardout, G. 2015: Ostracod-based palaeotemperature reconstructions for MIS 11 human occupation at Beeches Pit, West Stow, Suffolk, UK. *Journal of Archaeological Science* 54, 421–425.
- Berger, A. & Loutre, M.-F. 2003: Climate 400,000 years ago, a key to the future? In Droxler, A. W., Poore, R. Z. & Burckle, L. H. (eds.): *Earth's Climate and Orbital Eccentricity: The Marine Isotope Stage 11 Question*, 17–26. Geophysical Monograph, Washington.
- Berstad, M. I., Lundberg, J., Lauritzen, S.-E. & Linge, H. C. 2002: Comparison of the climate during marine isotope stage 9 and 11 inferred from a speleothem isotope record from northern Norway. *Quaternary Research* 58, 361–371.
- Bigga, G. 2018: Die Pflanzen von Schöningen. Botanische Makroreste aus den mittelpleistozänen Ablagerungen und das Nutzungspotential einer interglazialen Paläoflora. 304 pp. In *Forschungen zur Urgeschichte im Tagebau von Schöningen, Band 3*. Verlag des Römisch-Germanischen Zentralmuseums, Mainz.
- Bittmann, F. 2012: Die Schöninger Pollendiagramme und ihre Stellung im mitteleuropäischen Mittelpleistozän. In Behre, K.-E. (ed.): *Die chronologische Einordnung der paläolithischen Fundstellen von Schöningen*, 97–112. Verlag des Römisch-Germanischen Zentralmuseums, Mainz.
- Błaszyk, M. & Hercman, H. 2022: Palaeoclimate in the low Tatras of the Western Carpathians during MIS 11–6: insights from multiproxy speleothem records. *Quaternary Science Reviews* 275, 107290, <https://doi.org/10.1016/j.quascirev.2021.107290>.
- Böhme, G. 2015: Fische, Amphibien und Reptilien aus dem Mittelpleistozän (Reinsdorf-Interglazial) von Schöningen (II) bei Helmstedt (Niedersachsen). In Terberger, T. & Winghart, S. (eds.): *Die Geologie der paläolithischen Fundstellen von Schöningen. Forschungen zur Urgeschichte aus dem Tagebau Schöningen, Band 2*, 203–265. Verlag des Römisch-Germanischen Zentralmuseums, Mainz.
- Böhner, U., Fricke, C., Mania, D. & Thieme, H. 2005: *Schöningen 13 II, Referenzprofil. Stand April 2005. Dokumentationsdatenbank*. Niedersächsisches Landesamt für Denkmalpflege, Hannover.
- Brandes, C., Pollok, L., Schmidt, C., Wilde, V. & Winsemann, J. 2012: Basin modelling of a lignite-bearing salt rim syncline: insights into rim syncline evolution and salt diapirism in NW Germany. *Basin Research* 24, 699–716.
- Bridgland, D. R., Harding, P., Allen, P., Candy, I., Cherry, C., George, W., Horne, D., Keen, D. H., Penkman, K. E. H., Preece, R. C., Rhodes, E. J., Scaife, R., Schreve, D. C., Schwenninger, J.-L., Slipper, I., Ward, G., White, M. J., White, T. S. & Whittaker, J. E. 2013: An enhanced record of MIS 9 geoarchaeology: data from construction of the high speed 1 (London – channel tunnel) rail-link and other recent investigations at Purfleet, Essex, UK. *Proceedings of the Geologists' Association* 124, 417–476.
- Brodie, C. R., Casford, J. S. L., Lloyd, J. M., Leng, M. J., Heaton, T. H. E., Kendrick, C. P. & Yongqiang, Z. 2011: Evidence for bias in C/N, $\delta^{13}\text{C}$ and $\delta^{15}\text{N}$ values of bulk organic matter, and on environmental interpretation, from a lake sedimentary sequence by pre-analysis acid treatment methods. *Quaternary Science Reviews* 30, 3076–3087.
- Candy, I., Schreve, D. C., Sherriff, J. & Tye, G. J. 2014: Marine isotope stage 11: Palaeoclimates, palaeoenvironments and its role as an analogue for the current interglacial. *Earth-Science Reviews* 128, 18–51.

- Cohen, K. M. & Gibbard, P. L. 2016: *Global chronostratigraphical correlation table for the last 2.7 million years version 2019 QI-500*. International Commission on Stratigraphy, <http://www.stratigraphy.org/index.php/ics-chart-timescale>.
- Conard, N. J., Serangeli, J., Böhrer, U., Starkovich, B. M., Miller, C. E., Urban, B. & van Kolfschoten, T. 2015: Excavations at Schöningen and paradigm shifts in human evolution. *Journal of Human Evolution* 89, 1–17.
- Daniel, T. & Frenzel, P. 2023: Pleistocene freshwater ostracods from the Homo erectus site at Bilzingsleben, Germany—review of historic collection and unpublished manuscript material for palaeoenvironmental reconstruction. *Geoarchaeology* 38, 445–465.
- De Deckker, P. 2002: Ostracod Palaeoecology. In Holmes, J. A. & Chivas, A. R. (eds.): *The Ostracoda: Applications in Quaternary Research*, 121–134. Geophysical Monograph, Washington.
- Denys, L. 1990: Fragilaria blooms in the Holocene of western coastal plain of Belgia. In Simola, H. (ed.): *Proceedings of the 10th International Diatom Symposium*, 397–406. Koeltz Scientific Books, Königstein.
- Desprat, S., Sánchez Goñi, M. F., McManus, J., Duprat, J. & Cortijo, E. 2009: Millennial-scale climatic variability between 340 000 and 270 000 years ago in SW Europe: evidence from a NW Iberian margin pollen sequence. *Climate of the Past* 5, 53–72.
- Drysdale, R. N., Zanchetta, G., Hellstrom, J. C., Fallick, A. E., Zhao, J.-Z., Isola, I. & Bruschi, G. 2004: Palaeoclimatic implications of the growth history and stable isotope ($\delta^{18}\text{O}$ and $\delta^{13}\text{C}$) geochemistry of a middle to late Pleistocene stalagmite from central-western Italy. *Earth and Planetary Science Letters* 227, 215–229.
- Duckson, D. W. 1987: Continental climate. In Oliver, J. E. (ed.): *Encyclopedia of Earth Science*, 364–365. Springer, Boston, Massachusetts.
- DWD 1988–2022: Deutscher Wetterdienst. Available at: <https://cdc.dwd.de/portal/> (accessed 21.05.2023).
- DWD 2003–2022: Deutscher Wetterdienst. Available at: <https://cdc.dwd.de/portal/> (accessed 21.05.2023).
- Enters, D., Lücke, A. & Zolitschka, B. 2006: Effects of land-use change on deposition and composition of organic matter in Frickenhauser see, northern Bavaria, Germany. *Science of the Total Environment* 369, 178–187.
- Evers, M. 2017: *Charakteristika ausgewählter Abflüsse am Elmrand bei Schöningen*. Bachelor thesis, Technische Universität Braunschweig, 57 pp.
- Fernández Arias, S., Förster, M. W. & Sirocko, F. 2023: Rieden tephra layers in the Dottinger maar lake sediments: implications for the dating of the Holsteinian interglacial and Elsterian glacial. *Global and Planetary Change* 227, 104143, <https://doi.org/10.1016/j.gloplacha.2023.104143>.
- Fletcher, W. J., Müller, U. C., Koutsodendris, A., Christanis, K. & Pross, J. 2013: A centennial-scale record of vegetation and climate variability from 312 to 240 ka (marine isotope stages 9c-a, 8 and 7e) from Tenaghi Philippon, NE Greece. *Quaternary Science Reviews* 78, 108–125.
- Flower, R. J. 1993: Diatom preservation: experiments and observations on dissolution and breakage in modern and fossil material. *Hydrobiologia* 269/270, 473–484.
- Fuhrmann, R. 2012: *Atlas quartärer und rezenter Ostrakoden Mitteldeutschlands*. 320 pp. Naturkundliches Museum Mauretania, Altenburg.
- Gasse, F., Fontes, J.-C., Plaziat, J. C., Carbonel, P., Kaczmarek, I., De Dekker, P., Soulié-Marsche, I., Callot, Y. & Dupeuble, P. A. 1987: Biological remains, geochemistry and stable isotopes for the reconstruction of environmental and hydrological changes in the Holocene lakes from North Sahara. *Palaeogeography, Palaeoclimatology, Palaeoecology* 60, 1–46.
- Geyh, M. A. & Krbetschek, M. 2012: Zum radiometrischen Alter des Holstein-Interglazials. In Behre, K.-E. (ed.): *Die chronologische Einordnung der paläolithischen Fundstellen von Schöningen*, 155–170. Verlag des Römisch-Germanischen Zentralmuseums, Mainz.
- Geyh, M. A. & Müller, H. 2005: Numerical $^{230}\text{Th}/\text{U}$ dating and a palynological review of the Holsteinian/Hoxnian interglacial. *Quaternary Science Reviews* 24, 1861–1872.
- van Grafenstein, U., Erlenkeuser, H., Müller, J. & Kleinmann-Eisenmann, A. 1992: Oxygen isotope records of benthic ostracods in bavarian lake sediments. *Naturwissenschaften* 79, 145–152.
- van Grafenstein, U., Erlenkeuser, H. & Trimborn, P. 1999: Oxygen and carbon isotopes in modern fresh-water ostracod valves: assessing vital offsets and autecological effects of interest for palaeoclimate studies. *Palaeogeography, Palaeoclimatology, Palaeoecology* 148, 133–152.
- Hammarlund, D. & Buchardt, B. 1996: Composite stable isotope records from a late Weichselian lacustrine sequence at Grænge, Lolland, Denmark: evidence of Allerød and younger dryas environments. *Boreas* 26, 8–22.
- Hammarlund, D., Aravena, R., Barnekow, L., Buchardt, B. & Possnert, G. 1997: Multi-component carbon isotope evidence of early Holocene environmental change and carbon-flow pathways from a hard-water lake in northern Sweden. *Journal of Paleolimnology* 18, 219–233.
- Hammer, Ø., Harper, D. A. T. & Ryan, P. D. 2001: PAST: Palaeontological statistics software package for education and data analysis. *Palaeontologia Electronica* 4, 1–9. http://palaeo-electronica.org/2001_1/past/issue1_01.htm.
- Haworth, E. Y. 1976: Two late-glacial (late-Devensian) diatom assemblage profiles from northern Scotland. *New Phytologist* 77, 227–256.
- Hickman, M. & Reasoner, M. A. 1994: Diatom responses to late quaternary vegetation and climate change and to deposition of two tephras in an alpine and a subalpine lake in Yoho National Park, British Columbia. *Journal of Paleolimnology* 11, 173–188.
- Hickman, M. & Reasoner, M. A. 1998: Late quaternary diatom response to vegetation and climate change in a subalpine lake in Banff National Park, Alberta. *Journal of Paleolimnology* 20, 253–265.
- Horne, D. 2007: A mutual temperature range method for quaternary palaeoclimatic analysis using European nonmarine Ostracoda. *Quaternary Science Reviews* 26, 398–415.
- Horne, D. J., Curry, B. B. & Mesquita-Joanes, F. 2012: Mutual climatic range methods for quaternary ostracods. In Horne, D. J., Holmes, J. A., Rodriguez-Lazaro, J. & Viehberg, F. (eds.): *Ostracoda as Proxies for Quaternary Climate Change, Developments in Quaternary Sciences* 17, 65–84. Elsevier, Amsterdam.
- Horne, D. J., Ashton, N., Benardout, G., Brooks, S. J., Coope, G. R., Holmes, J. A., Lewis, S. G., Parfitt, S. A., White, T. S., Whitehouse, N. J. & Whittaker, J. E. 2023: A terrestrial record of climate variation during MIS 11 through multiproxy palaeotemperature reconstructions from Hoxne, UK. *Quaternary Research* 111, 21–52.
- IAEA/WMO 2022: Global network of isotopes in precipitation. The GNIP database. Available at: <http://www.iaea.org/water> (accessed 31.03.2022).
- Ito, E. 2001: Application of stable isotope techniques to inorganic and biogenic carbonates. In Last, W. M. & Smol, J. P. (eds.): *Tracking Environmental Change Using Lake Sediments. Volume 2: Physical and Geochemical Methods*, 351–371. Kluwer Academic Publishers, Dordrecht.
- Juggins, S. 2007: *User Guide C2 Software for Ecological and Palaeoecological Data Analysis and Visualization, User Guide Version 1.5*. 73 pp. Department of Geography, University of Newcastle, Newcastle upon Tyne.
- Kalbe, L. & Werner, H. 1974: Sediment des Kummerower Sees. Untersuchungen des Chemismus und der Diatomeenflora. *Internationale Revue der Gesamten Hydrobiologie* 56, 755–782.
- Kashima, K. 2003: The quantitative reconstruction of salinity changes using diatom assemblages in inland saline lakes in the central part of Turkey during the late Quaternary. *Quaternary International* 105, 13–19.
- Kern, O. A., Koutsodendris, A., Allstädt, F. J., Mächtle, B., Petzet, D. M., Kalaitzidis, S., Christanis, K. & Pross, J. 2022: A near-continuous record of climate and ecosystem variability in Central Europe during the past 130 kys (marine isotope stages 5–1) from Fürmoos, southern Germany. *Quaternary Science Reviews* 284, 107505, <https://doi.org/10.1016/j.quascirev.2022.107505>.
- Kleinmann, A., Müller, H., Lepper, J. & Waas, D. 2011: Nachtigall: a continental sediment and pollen sequence of the Saalian complex in NW-Germany and its relationship to the MIS-framework. *Quaternary International* 241, 97–110.
- van Kolfschoten, T. 2014: The Palaeolithic locality Schöningen (Germany): a review of the mammalian record. *Quaternary International* 326–327, 469–480.

- Koutsodendris, A., Müller, U. C., Pross, J., Brauer, A., Kotthoff, U. & Lotter, A. F. 2010: Vegetation dynamics and climate variability during the Holsteinian interglacial based on a pollen record from Dethlingen (northern Germany). *Quaternary Science Reviews* 29, 3298–3307.
- Koutsodendris, A., Brauer, A., Pälke, H., Müller, U. C., Dulski, P., Lotter, A. F. & Pross, J. 2011: Sub-decadal- to decadal-scale climate cyclicity during the Holsteinian interglacial (MIS 11) evidenced in annually laminated sediments. *Climate of the Past* 7, 987–999.
- Koutsodendris, A., Lotter, A. F., Kirilova, E., Verhagen, F. T. M., Brauer, A. & Pross, J. 2013: Evolution of a Holsteinian (MIS 11c) palaeolake based on a 12-kyr-long diatom record from Dethlingen (northern Germany). *Boreas* 42, 714–728.
- Koutsodendris, A., Dakos, V., Fletcher, W. J., Knipping, M., Kotthoff, U., Milner, A. M., Müller, U. C., Kaboth-Bahr, S., Kern, O. A., Kolb, L., Vakhrameeva, P., Wulf, S., Christanis, K., Schmiel, G. & Pross, J. 2023: Atmospheric CO₂ forcing on Mediterranean biomes during the past 500 kyrs. *Nature Communications* 14, 1664, <https://doi.org/10.1038/s41467-023-37388-x>.
- Krahn, K. J., Tucci, M., Urban, B., Pilgrim, J., Frenzel, P., Soulié-Marsche, I. & Schwalb, A. 2021: Aquatic and terrestrial proxy evidence for middle Pleistocene palaeolake and lakeshore development at two palaeolithic sites of Schöningen (Germany). *Boreas* 50, 723–745.
- Krammer, K. & Lange-Bertalot, H. 1986: Bacillariophyceae. 1. Teil: Naviculaceae. In Ettl, H., Gerloff, J., Heynig, H. & Mollenhauer, D. (eds.): *Süßwasserflora von Mitteleuropa, Band 2/1*. 876 pp. Gustav Fischer Verlag, Stuttgart.
- Krammer, K. & Lange-Bertalot, H. 1988: Bacillariophyceae. 2. Teil: Bacillariaceae, Epithemiaceae, Surirellaceae. In Ettl, H., Gerloff, J., Heynig, H. & Mollenhauer, D. (eds.): *Süßwasserflora von Mitteleuropa, Band 2/2*. 612 pp. Gustav Fischer Verlag, Stuttgart.
- Krammer, K. & Lange-Bertalot, H. 1991a: Bacillariophyceae. 3. Teil: Centrales, Fragilariaceae, Eunotiaceae. In Ettl, H., Gerloff, J., Heynig, H. & Mollenhauer, D. (eds.): *Süßwasserflora von Mitteleuropa, Band 2/3*. 576 pp. Gustav Fischer Verlag, Stuttgart.
- Krammer, K. & Lange-Bertalot, H. 1991b: Bacillariophyceae. 4. Teil: Achnantheaceae. Kritische Ergänzungen zu Navicula (Lineolatae) und Gomphonema. In Ettl, H., Gärtner, G., Gerloff, J., Heynig, H. & Mollenhauer, D. (eds.): *Süßwasserflora von Mitteleuropa, Band 2/4*. 437 pp. Gustav Fischer Verlag, Stuttgart.
- Lacey, J. H., Leng, M. J., Francke, A., Sloane, H. J., Milodowski, A., Vogel, H., Baumgarten, H., Zanchetta, G. & Wagner, B. 2016: Northern Mediterranean climate since the middle Pleistocene: a 637 ka stable isotope record from Lake Ohrid (Albania/Macedonia). *Biogeosciences* 13, 1801–1820.
- Lang, J., Winsemann, J., Steinmetz, D., Polom, U., Pollok, L., Böhner, U., Serangeli, J., Brandes, C., Hampel, A. & Winghart, S. 2012: The Pleistocene of Schöningen, Germany: a complex tunnel valley fill revealed from 3D subsurface modelling and shear wave seismics. *Quaternary Science Reviews* 39, 86–105.
- Lang, J., Böhner, U., Polom, U., Serangeli, J. & Winsemann, J. 2015: The middle Pleistocene tunnel valley at Schöningen as a Palaeolithic archive. *Journal of Human Evolution* 89, 18–26.
- Lange-Bertalot, H., Hofmann, G., Werum, M. & Cantonati, M. 2017: *Freshwater Benthic Diatoms of Central Europe: Over 800 Common Species Used in Ecological Assessment*. 942 pp. Koeltz Botanical Books, Schmitten-Oberreifenberg.
- Last, W. M. & Smol, J. P. 2001: *Tracking Environmental Change Using Lake Sediments Volume 2: Physical and Geochemical Methods*. 504 pp. Kluwer Academic Publishers, Dordrecht.
- Lauer, T. & Weiss, M. 2018: Timing of the Saalian- and Elsterian glacial cycles and the implications for middle–Pleistocene hominin presence in central Europe. *Scientific Reports* 8, 5111, <https://doi.org/10.1038/s41598-018-23541-w>.
- Leng, M. & Marshall, J. 2004: Palaeoclimate interpretation of stable isotope data from lake sediment archives. *Quaternary Science Reviews* 23, 811–831.
- Leng, M. J., Baneschi, I., Zanchetta, G., Jex, C. N., Wagner, B. & Vogel, H. 2010: Late quaternary palaeoenvironmental reconstruction from lakes Ohrid and Prespa (Macedonia/Albania border) using stable isotopes. *Biogeosciences* 7, 3109–3122.
- Lisiecki, L. E. & Raymo, M. E. A. 2005: Pliocene-Pleistocene stack of 57 globally distributed benthic ¹⁸O records. *Paleoceanography* 20, 1–17.
- Litt, T., Behre, K.-E., Meyer, K.-D., Stephan, H.-J. & Wansa, S. 2007: Stratigraphische Begriffe für das Quartär des norddeutschen Vereisungsgebietes. *Eiszeitalter und Gegenwart* 56, 7–65.
- Liu, W., Li, X., Wang, Z., Wang, H., Liu, H., Zhang, B. & Zhang, H. 2019: Carbon isotope and environmental changes in lakes in arid Northwest China. *Science China Earth Sciences* 62, 1193–1206.
- Löffler, H. 1959: Zur Limnologie. Entomotraken- und Rotatorienfauna des Seewinkelgebietes (Burgenland, Österreich). *Sitzungsberichte Österreichische Akademie der Wissenschaften, Mathematisch-Naturwissenschaftliche Klasse I* 168, 315–362.
- Lotter, A. F. & Bigler, C. 2000: Do diatoms in the Swiss Alps reflect the length of ice-cover? *Aquatic Sciences* 62, 125–141.
- Loutre, M. F. & Berger, A. 2003: Marine isotope stage 11 as an analogue for the present interglacial. *Global and Planetary Change* 36, 209–217.
- Lu, Y., Meyers, P. A., Eadie, B. J. & Robbins, J. A. 2010: Carbon cycling in Lake Erie during cultural eutrophication over the last century inferred from the stable carbon isotope composition of sediments. *Journal of Paleolimnology* 43, 261–272.
- Lüthi, D., Le Floch, M., Bereiter, B., Blunier, T., Barnola, J.-M., Siegenthaler, U., Raynaud, D., Jouzel, J., Fischer, H., Kawamura, K. & Stocker, T. F. 2008: High-resolution carbon dioxide concentration record 650,000–800,000 years before present. *Nature* 453, 379–382.
- Mangili, C., Brauer, A., Plessen, B., Dulski, P., Moscariello, A. & Naumann, R. 2010: Effects of detrital carbonate on stable oxygen and carbon isotope data from varved sediments of the interglacial Piànico palaeolake (southern Alps, Italy). *Journal of Quaternary Science* 25, 135–145.
- Mania, D. 1995: Die geologischen Verhältnisse im Gebiet von Schöningen. In Thieme, H. & Maier, R. (eds.): *Archäologische Ausgrabungen im Braunkohlentagebau Schöningen, Landkreis Helmstedt*, 33–43. Hahnsche Buchhandlung, Hannover.
- Mania, D. 1998: Zum Ablauf der Klimazyklen seit der Elstervereisung im Elbe-Saalegebiet. *Prähistoria Thuringica* 2, 5–21.
- Mania, D. 2007: Das Eiszeitalter und seine Spuren im Tagebau Schöningen. In Thieme, H. (ed.): *Die Schöninger Speere – Mensch und Jagd vor 400.000 Jahren*, 35–86. Theiss Verlag, Stuttgart.
- Mania, D. & Altermann, M. 2015: Das Quartär von Schöningen im nördlichen Harzvorland. In Terberger, T. & Winghart, S. (eds.): *Die Geologie der paläolithischen Fundstellen von Schöningen. Forschungen zur Urgeschichte aus dem Tagebau Schöningen, Band 2*, 1–190. Verlag des Römisch-Germanischen Zentralmuseums, Mainz.
- Marchegiano, M., Horne, D. J., Gliozzi, E., Francke, A., Wagner, B. & Ariztegui, D. 2020: Rapid late Pleistocene climate change reconstructed from a lacustrine ostracod record in central Italy (Lake Trasimeno, Umbria). *Boreas* 49, 739–750.
- Martrat, B., Grimalt, J., López Martínez, C., Cacho, I., Sierro, F., Flores, J., Zahn, R., Canals, M., Curtis, J. & Hodell, D. 2005: Abrupt temperature changes in the Western Mediterranean over the past 250,000 years. *Science* 306, 1762–1765.
- Martrat, B., Grimalt, J. O., Shackleton, N. J., de Abreu, L., Hutterli, M. A. & Stocker, T. F. 2007: Four climate cycles of recurring deep and surface water destabilizations on the Iberian margin. *Science* 317, 502–507.
- McKenzie, J. A. & Hollander, D. J. 1993: Oxygen-isotope record in recent carbonate sediments from Lake Greifen, Switzerland (1750–1986): application of continental isotopic indicator for evaluation of changes in climate and atmospheric circulation patterns. In Swart, P. K., Lohmann, K. C., McKenzie, J. & Savin, S. (eds.): *Climate Change in Continental Isotopic Records*, 101–112. American Geophysical Union, Washington DC.
- Meisch, C. 2000: *Freshwater Ostracoda of Western and Central Europe*. 522 pp. Spektrum Akademischer Verlag, Heidelberg.
- Meyers, P. A. 1994: Preservation of elemental and isotopic source identification of sedimentary organic matter. *Chemical Geology* 114, 289–302.
- Müller, H. 1974: Pollenanalytische Untersuchungen und Jahresschichtenzählungen an der holstein-zeitlichen Kieselgur von Munster-Breloh. *Geologisches Jahrbuch A* 21, 107–140.

- Musil, R. 2007: Die Pferde von Schöningen: Skelettreste einer ganzen Wildpferdherde. In Thieme, H. (ed.): *Die Schöninger Speere – Mensch und Jagd vor 400.000 Jahren*, 136–140. Theiss Verlag, Stuttgart.
- Nitychoruk, J., Bińka, K., Hoefs, J., Ruppert, H. & Schneider, J. 2005: Climate reconstruction for the Holsteinian interglacial in eastern Poland and its comparison with isotopic data from marine isotope stage 11. *Quaternary Science Reviews* 24, 631–644.
- Nitychoruk, J., Bińka, K., Ruppert, H. & Schneider, J. 2006: Holsteinian interglacial=marine isotope stage 11? *Quaternary Science Reviews* 25, 2678–2681.
- Past Interglacials Working Group of PAGES 2016: Interglacials of the last 800,000 years. *Reviews of Geophysics* 54, 162–219.
- Railsback, L., Gibbard, P., Head, M., Voarintsoa, N. R. & Toucanne, S. 2015: An optimized scheme of lettered marine isotope substages for the last 1.0 million years, and the climatostratigraphic nature of isotope stages and substages. *Quaternary Science Reviews* 111, 94–106.
- Regattieri, E., Zanchetta, G., Isola, I., Bajo, P., Boschi, C., Perchiazzi, N., Drysdale, R., Hellstrom, J., Francke, A. & Wagner, B. 2018: A MIS 9/MIS 8 speleothem record of hydrological variability from Macedonia (F.Y.R.O.M.). *Global and Planetary Change* 162, 39–52.
- Reille, M., de Beaulieu, J.-L., Svoboda, V., Andrieu-Ponel, V. & Goeury, C. 2000: Pollen analytical biostratigraphy of the last five climatic cycles from a long continental sequence from the Velay region (Massif Central, France). *Journal of Quaternary Science* 15, 665–685.
- Richter, D. & Krbetschek, M. 2015: Luminescence dating of the lower Palaeolithic occupation at Schöningen 13/I. *Journal of Human Evolution* 89, 46–56.
- Rigterink, S., Krahn, K. J., Kotrys, B., Urban, B., Heiri, O., Turner, F., Pannes, A. & Schwab, A. 2024: Chironomid-Inferred Summer Temperatures from the Middle Pleistocene Site Schöningen 13 II, Northern Germany. *Boreas* 53, 525–542, <https://doi.org/10.1111/bor.12658>.
- Roucoux, K. H., Tzedakis, P. C., de Abreu, L. & Shackleton, N. J. 2006: Climate and vegetation changes 180,000 to 345,000 years ago recorded in a deep-sea core off Portugal. *Earth and Planetary Science Letters* 249, 307–325.
- Ruddiman, W. F. 2007: The early anthropogenic hypothesis: challenges and responses. *Reviews of Geophysics* 45, RG4001, <https://doi.org/10.1029/2006RG000207>.
- Sadori, L., Koutsodendris, A., Panagiotopoulos, K., Masi, A., Bertini, A., Combourieu-Nebout, N., Francke, A., Kouli, K., Joannin, S., Mercuri, A. M., Peyron, O., Torri, P., Wagner, B., Zanchetta, G., Sinopoli, G. & Donders, T. H. 2016: Pollen-based paleoenvironmental and paleoclimatic change at Lake Ohrid (south-eastern Europe) during the past 500 ka. *Biogeosciences* 13, 1423–1437.
- Sanderman, J., Krull, E., Kuhn, T., Hancock, G., McGowan, J., Maddern, T., Fallon, S. & Steven, A. 2015: Deciphering sedimentary organic matter sources: insights from radiocarbon measurements and NMR spectroscopy. *Limnology and Oceanography* 60, 739–753.
- Schelske, C. L. & Hodell, D. A. 1991: Recent changes in productivity and climate of Lake Ontario detected by isotopic analysis of sediments. *Limnology and Oceanography* 36, 961–975.
- Schulz, M. & Paul, A. 2015: *Integrated Analysis of Interglacial Climate Dynamics (INTERDYNAMIC)*. 146 pp. Springer Briefs in Earth System Sciences, Cham.
- Schwab, A. 2003: Lacustrine ostracodes as stable isotope recorders of late-glacial and holocene environmental dynamics and climate. *Journal of Paleolimnology* 29, 265–351.
- Serangeli, J., Böhner, U., Hafmann, H. & Conard, N. J. 2012: Die pleistozänen Fundstellen von Schöningen – eine Einführung. In Behre, K.-E. (ed.): *Die chronologische Einordnung der paläolithischen Fundplätze von Schöningen*, 1–22. Verlag des Römisch-Germanischen Zentralmuseums, Mainz.
- Serangeli, J., Rodríguez-Álvarez, B., Tucci, M., Verheijen, I., Bigga, G., Böhner, U., Urban, B., van Kolfschoten, T. & Conard, N. J. 2018: The project Schöningen from an ecological and cultural perspective. *Quaternary Science Reviews* 198, 140–155.
- Sierralta, M., Frechen, M. & Urban, B. 2012: $^{230}\text{Th}/\text{U}$ dating results from opencast mine Schöningen. In Behre, K.-E. (ed.): *Die chronologische Einordnung der paläolithischen Fundstellen von Schöningen*, 143–154. Verlag des Römisch-Germanischen Zentralmuseums, Mainz.
- Sirocko, F., Seelos, K., Schaber, K., Rein, B., Dreher, F., Diehl, M., Lehne, R., Jäger, K., Krbetschek, M. & Degering, D. 2005: A late Eemian aridity pulse in central Europe during the last glacial inception. *Nature* 436, 833–836.
- Smol, J. P. 1983: Palaeophycology of high arctic lake near cape Herschel, Ellesmere Island. *Canadian Journal of Botany* 61, 2195–2204.
- Smol, J. P., Birks, H. J. B. & Last, W. M. 2001a: *Tracking Environmental Change Using Lake Sediments Volume 3: Terrestrial, Algal and Siliceous Indicators*. 371 pp. Kluwer Academic Publishers, Dordrecht.
- Smol, J. P., Birks, H. J. B. & Last, W. M. 2001b: *Tracking Environmental Change Using Lake Sediments, Volume 4: Zoological Indicators*. 217 pp. Kluwer Academic Publishers, Dordrecht.
- Stahlschmidt, M. C., Miller, C. E., Ligouis, B., Goldberg, P., Berna, F., Urban, B. & Conard, N. J. 2015: The depositional environments of Schöningen 13 II-4 and their archaeological implications. *Journal of Human Evolution* 89, 181–201.
- Stephan, H.-J., Urban, B., Lüttig, G., Menke, B. & Sierralta, M. 2011: *Palynologische, petrographische und geochronologische Untersuchungen an Ablagerungen der Leck-Warmzeit (spätes Mittelpleistozän) und begleitender Sedimente. Geologisches Jahrbuch Reihe A, Heft 160*. 80 pp. Schweizerbart'sche Verlagsbuchhandlung, Stuttgart.
- Strahl, J. 2019: Ergebnisse palynologischer Untersuchungen an der Forschungsbohrung Ummendorf 1/2012 und Vergleich mit anderen pollenstratigraphischen Untersuchungen im oberen Allertal. In Wansa, S., Strahl, J. & Rappsilber, I. (eds.): *Zur Geologie des Ummendorfer Kessels im oberen Allertal. Mitteilungen zu Geologie und Bergwesen von Sachsen-Anhalt, Band 20 – Forschungsbohrung Ummendorf 1/2012*, 41–92. Landesamt für Geologie und Bergwesen Sachsen-Anhalt, Halle.
- Talbot, M. R. 2001: Nitrogen isotopes in palaeolimnology. In Last, W. M. & Smol, J. P. (eds.): *Tracking Environmental Change Using Lake Sediments: Physical and Chemical Techniques*, 401–439. Kluwer Academic Publishers, Dordrecht.
- Teranes, J. L. & McKenzie, J. A. 2001: Lacustrine oxygen isotope record of 20th-century climate change in central Europe: evaluation of climatic controls on oxygen isotopes in precipitation. *Journal of Paleolimnology* 26, 131–146.
- Thieme, H. 1997: Lower Palaeolithic hunting spears from Germany. *Nature* 385, 807–810.
- Thieme, H. 2007: *Die Schöninger Speere – Mensch und Jagd vor 400.000 Jahren*. 248 pp. Theiss, Stuttgart.
- Thieme, H. & Mania, D. 1993: “Schöningen 12” ein mittelpleistozänes Interglazialvorkommen im Nordharzvorland mit paläolithischen Funden. *Ethnographisch-Archäologische Zeitschrift* 34, 610–619.
- Thompson, R. 2004: The role of paleoclimatic studies in assessing climate change. *Eos, Transactions of the American Geophysical Union* 85, 436.
- Tucci, M., Krahn, K. J., van Kolfschoten, T., Richter, D., Rodríguez-Álvarez, B., Verheijen, I., Serangeli, J., Lehmann, J., Degering, D., Schwab, A. & Urban, B. 2021: Evidence for severe environmental change within an elephant find horizon during the middle Pleistocene Reinsdorf sequence at the palaeolithic site Schöningen 13 II-2c3 and its age determination, Germany. *Palaeogeography, Palaeoclimatology, Palaeoecology* 241, 125–142.
- Tzedakis, P. C., Raynouad, D., McManus, J. F., Berger, A., Brovkin, V. & Kiefer, T. 2009: Interglacial diversity. *Nature Geoscience* 2, 751–755.
- Tzedakis, P. C., Hodell, D. A., Nehrbass-Ahles, C., Mitsui, T. & Wolff, E. W. 2022: Marine Isotope Stage 11c: An unusual interglacial. *Quaternary Science Reviews* 284, 107493, <https://doi.org/10.1016/j.quascirev.2022.107493>.
- Urban, B. 1995: Palynological evidence of younger middle Pleistocene Interglacials (Holsteinian, Reinsdorf and Schöningen) in the Schöningen open cast lignite mine (eastern Lower Saxony, Germany). *Mededelingen Rijks Geologische Dienst* 52, 175–185.
- Urban, B. 2007: Interglacial pollen records from Schöningen, north Germany. In Sirocko, F., Claussen, M., Sánchez Goni, M. F. & Litt, T. (eds.): *The Climate of Past Interglacials*, 417–444. Elsevier, Amsterdam.

- Urban, B. & Bigga, G. 2015: Environmental reconstruction and biostratigraphy of late middle Pleistocene lakeshore deposits at Schöningen. *Journal of Human Evolution* 89, 57–70.
- Urban, B. & Thieme, H. 1991: Klima- und Landschaftsentwicklung im Eiszeitalter. Ergebnisse aus dem Tagebau Schöningen. *Mitteilungen, Braunschweigische Kohlen-Bergwerke AG Helmstedt und Tochtergesellschaften 1991/1*, 3–8.
- Urban, B., Thieme, H. & Elsner, H. 1988: Biostratigraphische, quartärgeologische und urgeschichtliche Befunde aus dem Tagebau "Schöningen", Landkreis Helmstedt. *Zeitschrift der Deutschen Geologischen Gesellschaft* 139, 123–154.
- Urban, B., Lenhard, R., Mania, D. & Albrecht, B. 1991: Mittelpleistozän im Tagebau Schöningen, Ldkr. Helmstedt. *Zeitschrift der Deutschen Geologischen Gesellschaft* 142, 351–372.
- Urban, B., Sierralta, M. & Frechen, M. 2011: New evidence for vegetation development and timing of upper middle Pleistocene interglacials in northern Germany and tentative correlations. *Quaternary International* 241, 125–142.
- Urban, B., Kasper, T., Krahn, K. J., Van Kolschoten, T., Rech, B., Holzheu, M., Tucci, M. & Schwalb, A. 2023a: Landscape dynamics and chronological refinement of the middle Pleistocene Reinsdorf sequence of Schöningen, NW Germany. *Quaternary Research* 114, 148–177.
- Urban, B., Krahn, K. J., Kasper, T., Garcia-Moreno, A., Hutson, J. M., Villaluenga, A., Turner, E., Gaudzinski-Windheuser, S., Farghaly, D., Tucci, M. & Schwalb, A. 2023b: Spatial interpretation of high-resolution environmental proxy data of the middle Pleistocene Palaeolithic faunal kill site Schöningen 13 II-4, Germany. *Boreas* 52, 440–458.
- Voormolen, B. 2008: *Ancient Hunters, Modern Butchers: Schöningen 13 II-4, a Kill-Butchery Site Dating from the Northwest European Lower Palaeolithic*. Doctoral thesis, University Leiden, 145 pp.
- Waas, D., Kleinmann, A. & Lepper, J. 2011: Uranium-series dating of fenpeat horizons from pit Nachtigall in northern Germany. *Quaternary International* 241, 111–124.
- Wansa, S., Strahl, J. & Rappsilber, I. 2019: Fazit der Untersuchungen im Ummendorfer Kessel. In Wansa, S., Strahl, J. & Rappsilber, I. (eds.): *Zur Geologie des Ummendorfer Kessels im oberen Allertal. Mitteilungen zu Geologie und Bergwesen von Sachsen-Anhalt, Band 20 – Forschungsbohrung Ummendorf 1/2012*, 201–204. Landesamt für Geologie und Bergwesen Sachsen-Anhalt, Halle.
- Weckström, K. & Juggins, S. 2005: Coastal diatom-environment relationships from the Gulf of Finland, Baltic Sea. *Journal of Phycology* 42, 21–35.
- Wrozyna, C., Frenzel, P., Steeb, P., Zhu, L. P. & Schwalb, A. 2009: Recent lacustrine Ostracoda and a first transfer function for palaeo-water depth estimation in Nam Co, southern Tibetan plateau. *Revista Española de Micropalaeontología* 41, 1–20.
- Xu, H., Li, A., Tan, L. & An, Z. 2006: Stable isotope in bulk carbonates and organic matter in recent sediments of Lake Qinghai and their climatic implications. *Chemical Geology* 235, 262–275.
- Yin, Q. & Berger, A. 2015: Interglacial analogues of the Holocene and its natural near future. *Quaternary Science Reviews* 120, 28–46.

Supporting Information

Additional Supporting Information to this article is available at <http://www.boreas.dk>.

Fig. S1. Most abundant ostracod and diatom taxa throughout the Reinsdorf sequence (PRP 13 II (2014) + ZB 13 II (2018)).

Fig. S2. Example of the application of the MOTR method on sample ZB23 of sequence RP 13 II (2014) + ZB (2018) which represents Reinsdorf C (Z-V). Results: mean January air temperature range $-4-0$ °C, mean July air temperature range $+17-19$ °C.

Table S1. Calibration for Mutual Ostracod Temperature Range method with mean monthly air temperature ranges in °C for January and July, respectively (Horne et al. 2012; D. J. Horne unpublished data) of the 22 calibrated species.